[10] Tomita T, Masuzaki H, Noguchi M, et al. GPR40 gene expression in human pancreas and insulinoma. Biochem Biophys Res Commun 2005;338:1788–90.
[11] Overton HA, Babbs AJ, Doel SM, et al. Deorphanization of a G protein-coupled receptor for oleoylethanolamide and its use in the discovery of small-molecule hypophagic agents. Cell Metab 2006;3:167–75.
[12] Lauffer LM, Iakoubov R, Brubaker PL. GPR119 is essential for oleoylethanolamide-induced glucagon-like peptide-1 secretion from the intestinal enteroendocrine L-cell. Diabetes 2009;58:1058–66.
[13] Hansen KB, Rosenkilde MM, Knop FK, et al. 2-Oleoyl glycerol is a GPR119 agonist and signals GLP-1 release in humans. J Clin Endocrinol Metab 2011;96:E1409–17, http://dx.doi.org/10.1210/jc.2011-0647.
[14] Chu ZL, Carroll C, Chen R, et al. N-oleoyldopamine enhances glucose homeostasis through the activation of GPR119. Mol Endocrinol 2010;24:161–70, http://dx.doi.org/10.1210/me.2009-0239.
[15] Soga T, Ohishi T, Matsui T, et al. Lysophosphatidylcholine enhances glucose-dependent insulin secretion via an orphan G-protein-coupled receptor. Biochem Biophys Res Commun 2005;326:744–51.
[16] Kogure R, Toyama K, Hiyamuta S, et al. 5-Hydroxy-eicosapentaenoic acid is an endogenous GPR119 agonist and enhances glucose-dependent insulin secretion. Biochem Biophys Res Commun 2011;416:58–63, http://dx.doi.org/10.1016/j.bbrc.2011.10.141.
[17] Ning Y, O'Neill K, Lan H, et al. Endogenous and synthetic agonists of GPR119 differ in signalling pathways and their effects on insulin secretion in MIN6c4 insulinoma cells. Br J Pharmacol 2008;155:1056–65.
[18] Chu ZL, Jones RM, He H, et al. A role for beta-cell-expressed G protein-coupled receptor 119 in glycemic control by enhancing glucose-dependent insulin release. Endocrinology 2007;148:2601–9.
[19] Chu ZL, Carroll C, Alfonso J, et al. A role for intestinal endocrine cell-expressed G protein-coupled receptor 119 in glycemic control by enhancing glucagon-like peptide-1 and glucose-dependent insulinotropic peptide release. Endocrinology 2008;149:2038–47.
[20] Lan H, Lin HV, Wang CF, et al. Agonists at GPR119 mediate secretion of GLP-1 from mouse enteroendocrine cells through glucose-independent pathways. Br J Pharmacol 2012;165:2799–807, http://dx.doi.org/10.1111/j.1476-5381.2011.01754.x.
[21] Semple G, Fioravanti B, Pereira G, et al. Discovery of the first potent and orally efficacious agonist of the orphan G-protein coupled receptor 119. J Med Chem 2008;51:5172–5.
[22] Lan H, Vassileva G, Corona A, et al. GPR119 is required for physiological regulation of glucagon-like peptide-1 secretion but not for metabolic homeostasis. J Endocrinol 2009;201:219–30.
[23] Gao J, Tian L, Weng G, et al. Stimulating beta-cell replication and improving islet graft function by AR231453, A gpr119 agonist. Transplant Proc 2011;43:3217–20, http://dx.doi.org/10.1016/j.transproceed.2011.10.021.
[24] Flock G, Holland D, Seino Y, et al. GPR119 regulates murine glucose homeostasis through incretin receptor-dependent and independent mechanisms. Endocrinology 2011;152:374–83.
[25] Semple G, Ren A, Fioravanti B, et al. Discovery of fused bicyclic agonists of the orphan G-protein coupled receptor GPR119 with in vivo activity in rodent models of glucose control. Bioorg Med Chem Lett 2011;21:3134–41, http://dx.doi.org/10.1016/j.bmcl.2011.03.007.
[26] Semple G, Lehmann J, Wong A, et al. Discovery of a second generation agonist of the orphan G-protein coupled receptor GPR119 with an improved profile. Bioorg Med Chem Lett 2011;22:1750–5, http://dx.doi.org/10.1016/j.bmcl.2011.12.092.
[27] Yoshida S, Ohishi T, Matsui T, et al. The role of small molecule GPR119 agonist, AS1535907, in glucose-stimulated insulin secretion and pancreatic beta-cell function. Diabetes Obes Metab 2011;13:34–41, http://dx.doi.org/10.1111/j.1463-1326.2010.01315.x.
[28] Cox HM, Tough IR, Woolston AM, et al. Peptide YY is critical for acylethanolamine receptor Gpr119-induced activation of gastrointestinal mucosal responses. Cell Metab 2010;11:532–42, http://dx.doi.org/10.1016/j.cmet.2010.04.014.
[29] Katz LB, Gambale JJ, Rothenberg PL, et al. Pharmacokinetics, pharmacodynamics, safety, and tolerability of JNJ-38431055, a novel GPR119 receptor agonist and potential antidiabetes agent, in healthy male subjects. Clin Pharmacol Ther 2011;90:685–92, http://dx.doi.org/10.1038/clpt.2011.169.
[30] Katz LB, Gambale JJ, Rothenberg PL, et al. Effects of JNJ-38431055, a novel GPR119 receptor agonist, in randomized, double-blind, placebo-controlled studies in subjects with type 2 diabetes. Diabetes Obes Metab 2012;14:709–16, http://dx.doi.org/10.1111/j.1463-1326.2012.01587.x; 10.1111/j.1463-1326.2012.01587.x.
[31] Vassilopoulos S, Esk C, Hoshino S, et al. A role for the CHC22 clathrin heavy-chain isoform in human glucose metabolism. Science 2009;324:1192–6.
[32] Seino Y, Nanjo K, Tajima N, et al. Report of the Committee on the Classification and diagnostic Criteria of Diabetes Mellitus. Diabetol Int 2010;1:2–20.
[33] Iwakura H, Hosoda K, Son C, et al. Analysis of rat insulin II promoter-ghrelin transgenic mice and rat glucagon promoter-ghrelin transgenic mice. J Biol Chem 2005;280:15247–56.
[34] Miyazaki J, Araki K, Yamato E, et al. Establishment of a pancreatic beta cell line that retains glucose-inducible insulin secretion: special reference to expression of glucose transporter isoforms. Endocrinology 1990;127:126–32.
[35] Ferrannini E, Gastaldelli A, Miyazaki Y, et al. beta-Cell function in subjects spanning the range from normal glucose tolerance to overt diabetes: a new analysis. J Clin Endocrinol Metab 2005;90:493–500.
[36] Matthews DR, Hosker JP, Rudenski AS, et al. Homeostasis model assessment: insulin resistance and beta-cell function from fasting plasma glucose and insulin concentrations in man. Diabetologia 1985;28:412–9.
[37] Briscoe CP, Tadayyon M, Andrews JL, et al. The orphan G protein-coupled receptor GPR40 is activated by medium and long chain fatty acids. J Biol Chem 2003;278:11303–11.
[38] Rajan AS, Aguilar-Bryan L, Nelson DA, et al. Sulfonylurea receptors and ATP-sensitive K+ channels in clonal pancreatic alpha cells. Evidence for two high affinity sulfonylurea receptors. J Biol Chem 1993;268:15221–8.
[39] Gribble FM, Reimann F. Sulphonylurea action revisited: the post-cloning era. Diabetologia 2003;46:875–91.
[40] Cooperberg BA, Cryer PE. Beta-cell-mediated signaling predominates over direct alpha-cell signaling in the regulation of glucagon secretion in humans. Diabetes Care 2009;32:2275–80.
[41] Rodriguez de Fonseca F, Navarro M, Gomez R, et al. An anorexic lipid mediator regulated by feeding. Nature 2001;414:209–12.
[42] Dockray GJ. The versatility of the vagus. Physiol Behav 2009;97:531–6.
[43] Engelstoft MS, Egerod KL, Holst B, et al. A gut feeling for obesity: 7TM sensors on enteroendocrine cells. Cell Metab 2008;8:447–9.
[44] Imagawa A, Hanafusa T, Uchigata Y, et al. Different contribution of class II HLA in fulminant and typical autoimmune type 1 diabetes mellitus. Diabetologia 2005;48:294–300.

Hindawi Publishing Corporation
International Journal of Endocrinology
Volume 2013, Article ID 590569, 5 pages
http://dx.doi.org/10.1155/2013/590569

Clinical Study

Past Obesity as well as Present Body Weight Status Is a Risk Factor for Diabetic Nephropathy

Shu Meguro,[1,2] Yusuke Kabeya,[2] Karin Tanaka,[1] Toshihide Kawai,[1] Masuomi Tomita,[2] Takeshi Katsuki,[2] Yoichi Oikawa,[2] Yoshihito Atsumi,[2,3] Akira Shimada,[2] Masami Tanaka,[1] Junichiro Irie,[1] Yoshifumi Saisho,[1] and Hiroshi Itoh[1]

[1] *Division of Endocrinology, Metabolism and Nephrology, Department of Internal Medicine, Keio University, School of Medicine, 35 Shinanomachi, Shinjuku-ku, Tokyo 160-8582, Japan*
[2] *Department of Internal Medicine, Saiseikai Central Hospital, Tokyo, Japan*
[3] *Diabetes Centre, Eiju General Hospital, Tokyo, Japan*

Correspondence should be addressed to Shu Meguro; shumeg@z8.keio.jp

Received 26 June 2013; Accepted 26 July 2013

Academic Editor: Ilias Migdalis

Aims. We analyzed the prevalence of nephropathy according to past body weight status in Japanese subjects with type 2 diabetes because the influence of past obesity on diabetic complications is not certain. *Methods.* We examined the prevalence of nephropathy in 2927 subjects with type 2 diabetes mellitus according to current BMI and maximum BMI in the past. We defined "current obesity" as BMI on hospitalization of 25 or more, "previous obesity" as BMI on hospitalization of less than 25 and self-reported maximum BMI in the past of 25 or more, and "continuously lean" as maximum BMI of less than 25. *Results.* The prevalence of nephropathy was significantly higher in subjects with current obesity (40.6%) or previous obesity (35.6%) than in those who were continuously lean (24.3%) ($P < 0.017$). In logistic regression analysis, previous obesity, as well as current obesity, was a significant risk factor for nephropathy, independent of sex, age, disease duration, hypertension, dyslipidemia, HbA1c, and diabetic retinopathy. *Conclusions.* Obesity in the past, as well as the present body weight status, was a risk factor for diabetic nephropathy.

1. Introduction

The majority of Japanese patients with type 2 diabetes mellitus are not obese, as reported by Kosaka and Ogata more than 50 years ago [1]. This is a well-known fact about Japanese type 2 diabetes mellitus [2]. Eastern Asian subjects might share common characteristics of the disease, comparable to those reported in Korean people [3]. It is, therefore, debatable whether we can apply epidemiological evidence obtained from studies of Caucasian subjects with type 2 diabetes and obesity to eastern Asian people, especially in the fields of diabetic complications, which are influenced not only by hyperglycemia but also by obesity. For example, type 2 diabetes is a relative risk factor for cardiovascular disease in Asians, as in Western societies, but the absolute risk differs greatly between these populations [4–7].

Recently, the "legacy effect" of intensive glycemic control early after the diagnosis of diabetes was advocated based on the UKPDS follow-up study [8]. However, there is no report about the legacy effect of past obesity over a lifetime on diabetic complications. Although there have been inconsistent results as to whether obesity is a risk for diabetic nephropathy [9–12], it was reported that current obesity and maximum past body mass index (BMI) were significant risk factors for diabetic nephropathy in the Japanese [12]. Although Caucasian subjects with type 2 diabetes usually maintain their body weight status during their disease course, the majority of patients of eastern Asian ethnicity begin to lose body weight from around the time of diagnosis of diabetes [3, 13]. This was easily overlooked, even if the effect of obesity in the past persisted for a long time, because they were already nonobese at the start of clinical follow-up. To clarify the influence of

past obesity on diabetic complications is an important clinical concern in patients of eastern Asian ethnicity.

We therefore analyzed the difference in the prevalence of diabetic nephropathy in Japanese type 2 diabetics according to their history of body weight status to clarify the effect of past obesity on diabetic nephropathy.

2. Materials and Methods

We examined subjects with type 2 diabetes whose estimated glomerular filtration rate (eGFR) was 30 mL/min/1.73 m^2 or more and who were admitted to Saiseikai Central Hospital from January 1999 to December 2004 ($n = 1834$) or Keio University Hospital from April 1998 to September 2010 ($n = 1093$) for the management of metabolic control. The study protocol was reviewed and approved by the ethics committee of both hospitals. Those subjects in whom the etiology of renal disease was strongly suspected to be other than diabetic nephropathy were excluded. According to the history of body weight status and the Japanese criteria for obesity [14], we defined "current obesity" as BMI on hospitalization of 25 or more, "previous obesity" as BMI on hospitalization of less than 25 and self-reported maximum BMI in the past of 25 or more, and "continuously lean" as maximum BMI of less than 25.

HbA1c level on admission was determined by high-performance liquid chromatography (HPLC: Arkray Inc., Kyoto, Japan) according to the recommended method by the Japan Diabetes Society (JDS) at that time and converted to the National Glycohemoglobin Standardization Program (NGSP) value [15]. eGFR (mL/min/1.73 m^2) was calculated as $194 \times Cr^{-1.094} \times Age^{-0.287}$ (with further multiplication by 0.739 for female subjects) using the equation provided by the Japanese Society of Nephrology [16].

Subjects with albumin excretion rate (AER) of 20 μg/min or more in 24-hour urine were considered to have diabetic nephropathy. All subjects underwent funduscopic examination by trained ophthalmologists during or just before admission. The diagnosis of diabetic retinopathy was made based on the Davis classification [17]. Hypertension was defined as systolic blood pressure >140 mmHg, diastolic blood pressure >90 mmHg, or the prescription of antihypertensive medication. Dyslipidemia was defined as LDL cholesterol >3.63 mmol/L, triglyceride >1.72 mmol/L, HDL cholesterol <1.04 mmol/L, or the prescription of lipid-lowering medication.

Continuous variables are expressed as mean ± SD. Differences in baseline characteristics among the obesity categories were analyzed by ANOVA and chi-squared test. Chi-squared test was also performed to evaluate differences in prevalence, with Bonferroni's correction for post hoc multiple comparisons. As a result, the probability equivalent to the usual $P = 0.05$ was $P = 0.017$. Logistic regression analysis with forced entry method was performed to detect significant independent predictors of diabetic nephropathy. We adopted as covariates factors such as sex, age, disease duration, hypertension, dyslipidemia, HbA1c, and obesity status (current obesity, past obesity, and continuously lean) in this study. Obesity status was converted to two dichotomous variables with dummy coding. $P < 0.05$ was considered statistically significant. All analyses were performed using IBM SPSS software ver. 18.0 (SPSS Inc., an IBM company, Japan).

3. Results

We analyzed a total of 2927 persons (males 2038, females 889, age 59.3 ± 10.6 years, BMI 24.0 ± 4.0, duration of diabetes 10.4 ± 28.0 years, HbA1c 9.3 ± 2.8%). The subjects' characteristics are shown in Table 1. The prevalence of current obesity in the total subjects was 33.6%, previous obesity 41.5%, and a continuous lean state 24.8%. The prevalence of nephropathy was significantly different among the categories, and both currently obese (40.6%) and previously obese (35.6%) patients had a significantly higher prevalence of diabetic nephropathy than that in continuously lean patients (24.3%) ($P < 0.017$).

When we divided the patients into quartiles according to current BMI, the prevalence of nephropathy significantly increased as current BMI increased (Figure 1, $P < 0.001$). When we similarly divided them into quartiles according to previous maximum BMI, the prevalence of nephropathy significantly increased as previous maximum BMI increased (Figure 1, $P < 0.001$). Current BMI and previous maximum BMI were highly correlated with each other ($r = 0.785$, $P < 0.001$).

In logistic regression analysis, both current obesity and previous obesity revealed a significant odds ratio for nephropathy, as well as diabetic retinopathy, independent of sex, age, disease duration, hypertension, dyslipidemia, and HbA1c (Table 2).

4. Discussion

We confirmed that previous obesity, as well as present obesity, was closely associated with nephropathy in type 2 diabetes. The notable finding of this study was that obesity is an independent risk factor, not only if it is present, but also if it was present in the past. This might indicate a legacy effect of obesity on nephropathy. The mechanism is the theme for investigation of how obesity in the past can influence diabetic complications over time.

Both current BMI and previous maximum BMI were associated with the nephropathy, as demonstrated in Figure 1. However, current BMI and previous maximum BMI were highly correlated with each other. So, generally, the higher the previous BMI, the higher the current BMI. When we analyzed the effects of previous obesity, we had to separate the effects of current obesity from those of previous obesity. This was the reason we analyzed the effect of previous obesity according to the categories defined as previous maximum BMI and current BMI. As a result, we could elucidate the effect of previous obesity on diabetic nephropathy.

Whether nephropathy in type 2 diabetes really derives from diabetes has always been a point of discussion. However, type 2 diabetes *per se* is a disease so closely linked with obesity and the metabolic syndrome that we cannot strictly distinguish the cause among the components of the syndrome. We here found that the effect of obesity was independent of the

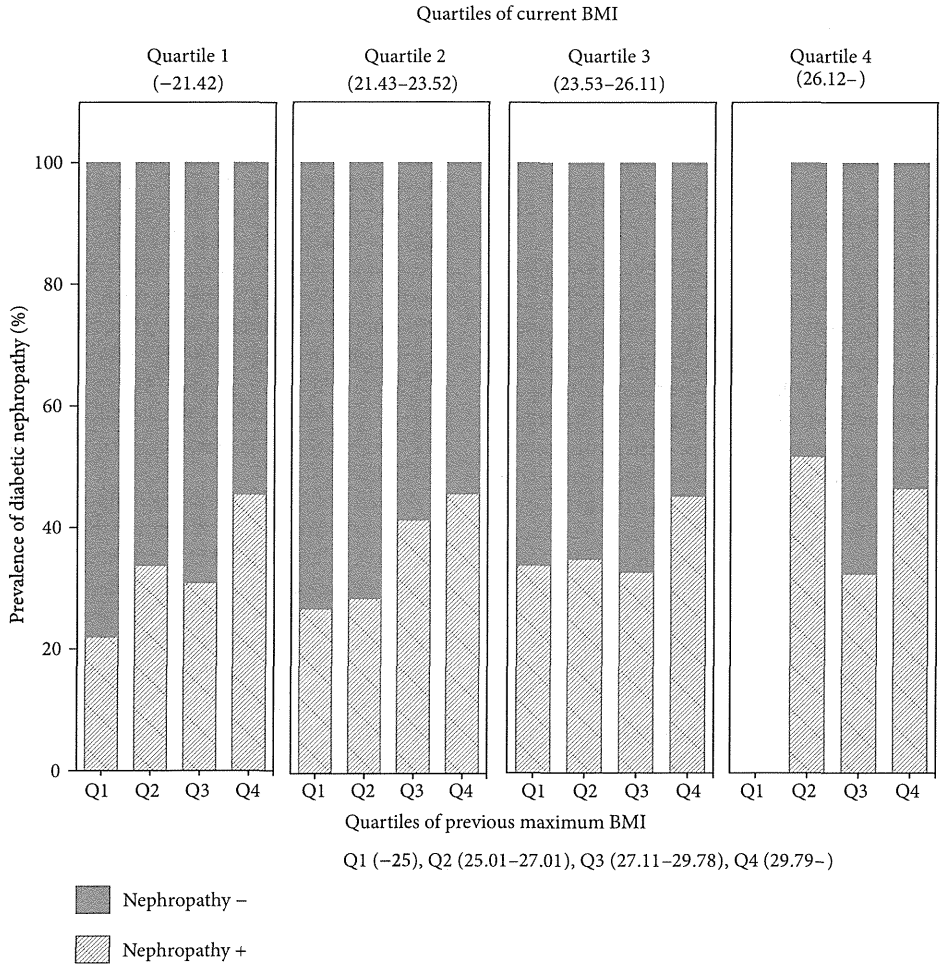

FIGURE 1: Prevalence of diabetic nephropathy divided by quartiles of current BMI and quartiles of previous maximum BMI. As for quartiles of current BMI, Quartile 1; BMI ≦ 21.42, Quartile 2; BMI: 21.43–23.52, Quartile 3; BMI: 23.53–26.11, and Quartile 4; BMI > 26.11. As for quartiles of previous maximum BMI, Quartile 1 (Q1); BMI ≦ 25.00, Quartile 2 (Q2); BMI: 25.01–27.10, Quartile 3 (Q3); BMI: 27.11–29.78, and Quartile 4 (Q4); BMI > 29.78. Prevalence of diabetic nephropathy was significantly different among the quartile groups of current BMI ($P < 0.001$ by chi-squared analysis). Prevalence of diabetic nephropathy was significantly different among the quartile groups of previous maximum BMI ($P < 0.001$ by chi-squared analysis).

existence of diabetic retinopathy, and we expect this result can be applied to all type 2 diabetes patients.

Several groups, including us, have reported that albuminuria was the strongest predictor of the progression of diabetic nephropathy [18–22]. We did not chronologically follow the decline of glomerular filtration rate (GFR) in this study. However, as we defined diabetic nephropathy by albuminuria, obesity, either current or past, might relate to the GFR decline through albuminuria.

Recently, the concept of obesity-related nephropathy has been advocated [23]. Although this concept is strictly defined with exclusion of both nephrosclerosis and diabetic nephropathy, the suspected mechanisms, including the contraction of efferent glomerular arterioles by the activated renin-angiotensin system (RAS) and glomerular hyperfiltration, as well as glomerular hypertrophy due to insulin resistance, are very similar to those of diabetic nephropathy. The border between the concepts of diabetic nephropathy and obesity-related nephropathy is unclear, and they cannot be distinguished clinically if a patient has both. Vivante et al. reported that overweight state and obesity in adolescents were associated with significantly increased risk for both diabetic and nondiabetic ESRD during a 25-year period [24]. If obesity even before the diagnosis of diabetes influences kidney function later, these concepts are continuous and indivisible.

There are some limitations of this study. One is that this study was retrospective, based on self-reported body weight in the past. As for the other limitation, we might have to consider how they lost their body weight because the study subjects required metabolic interventions for poor glycemic status. The duration of obesity must be a factor of interest affecting the results. However, we only have the data of maximum body weight and the body weight on admission but

Table 1: Characteristics of study subjects.

	Total	Continuously lean	Previous obesity	Current obesity	P value
Age	59.3 ± 10.6	61.1 ± 9.4	60.4 ± 10.0	56.7 ± 11.6	<0.01
Sex (male/female)	2038/889	486/243	870/345	682/301	ns
BMI	24.0 ± 4.0	20.5 ± 2.1	22.6 ± 1.7	28.3 ± 3.2	<0.01
Max. BMI	27.7 ± 4.3	23.0 ± 1.7	27.5 ± 2.3	31.4 ± 4.1	<0.01
Disease duration (years)	10.4 ± 28.0	10.4 ± 8.4	12.2 ± 42.2	8.2 ± 7.8	<0.01
SBP (mmHg)	132 ± 18	131 ± 17	132 ± 18	133 ± 18	ns
DBP (mmHg)	75 ± 11	74 ± 11	75 ± 11	75 ± 10	ns
FPG (mmol/L)	9.9 ± 4.0	9.5 ± 4.0	9.9 ± 4.1	10.2 ± 3.9	ns
HbA1c (%)	9.3 ± 2.8	9.1 ± 2.7	9.5 ± 3.4	9.3 ± 2.0	<0.05
TC (mmol/L)	5.3 ± 1.2	5.3 ± 1.0	5.2 ± 1.0	5.5 ± 1.6	<0.01
HDL (mmol/L)	1.3 ± 0.5	1.5 ± 0.5	1.3 ± 0.4	1.2 ± 0.3	<0.01
TG (mmol/L)	1.6 ± 1.4	1.4 ± 0.2	1.5 ± 1.1	1.9 ± 1.6	<0.01
Cr (mmol/L)	66.3 ± 19.4	64.5 ± 16.8	66.3 ± 19.4	68.9 ± 20.3	<0.01
eGFR (mL/min/1.73 m^2)	81.8 ± 28.8	81.4 ± 20.5	83.1 ± 31.1	80.6 ± 31.0	ns
Retinopathy (none/simple/proliferative)	2111/505/311	558/116/55	824/225/166	729/164/90	<0.01

Continuous variables are expressed as mean ± SD. Differences in baseline characteristics among the obesity categories were analyzed by ANOVA and chi-squared test. The numbers of each stage of diabetic retinopathy are noted on the row of retinopathy. SBP: systolic blood pressure, DBP: diastolic blood pressure, FPG: fasting blood glucose, TC: total cholesterol, HDL: HDL cholesterol, TG: triglyceride, ns: not significant.

Table 2: Logistic regression analysis with forced entry method for diabetic nephropathy.

	Odds ratio	95% confidence interval	P value
Age	1.011	1.002–1.019	<0.05
Disease duration	1.001	0.998–1.004	ns
Sex (male: 1, female: 0)	1.955	1.606–2.378	<0.001
Hypertension	1.232	1.023–1.484	<0.05
Dyslipidemia	1.306	1.096–1.556	<0.01
HbA1c	1.014	0.984–1.044	ns
Diabetic retinopathy	3.856	3.214–4.626	<0.001
Previous obesity: 1, other: 0	1.656	1.323–2.073	<0.001
Current obesity: 1, other: 0	2.480	1.959–3.141	<0.001

Adjusted $R^2 = 0.166$, $P < 0.001$. ns: not significant.

not the duration. So the hypothesis needs to be confirmed in a future large cohort study with more detailed information. In spite of these limitations, this was an analysis of a large population over 10 years. We therefore believe it includes important suggestions on the effect of obesity on diabetic nephropathy.

5. Conclusion

Our study indicated that obesity in the past, as well as present obesity, was a risk factor for diabetic nephropathy. We should consider the effect of earlier obesity on diabetic nephropathy even if it has been present before the diagnosis of diabetes.

Acknowledgments

The authors thank Ms. E. Inoue, and all the staff at Keio University Hospital for their assistance. They also thank all the staff at Saiseikai Central Hospital for their assistance.

References

[1] K. Kosaka and Y. Ogata, "Obesity and diabetes mellitus," *Saishin Igaku*, vol. 16, no. 10, pp. 2602–2608, 1961 (Japanese).

[2] H. Sone, Y. Yoshimura, H. Ito, Y. Ohashi, and N. Yamada, "Energy intake and obesity in Japanese patients with type 2 diabetes," *The Lancet*, vol. 363, no. 9404, pp. 248–249, 2004.

[3] J. Y. Park, K. Lee, C. H. Kim et al., "Past and current obesity in Koreans with non-insulin-dependent diabetes mellitus," *Diabetes Research and Clinical Practice*, vol. 35, no. 1, pp. 49–56, 1997.

[4] T. Nishimura, K. Nakajima, H. Kusuoka, A. Yamashina, and S. Nishimura, "Prognostic study of risk stratification among Japanese patients with ischemic heart disease using gated myocardial perfusion SPECT: J-ACCESS study," *European Journal of Nuclear Medicine and Molecular Imaging*, vol. 35, no. 2, pp. 319–328, 2008.

[5] M. Haffner, S. Lehto, T. Rönnemaa, K. Pyörälä, and M. Laakso, "Mortality from coronary heart disease in subjects with type 2 diabetes and in nondiabetic subjects with and without prior myocardial infarction," *The New England Journal of Medicine*, vol. 339, no. 4, pp. 229–234, 1998.

[6] H. Sone, S. Tanaka, S. Iimuro et al., "Long-term lifestyle intervention lowers the incidence of stroke in Japanese patients with type 2 diabetes: a nationwide multicentre randomised controlled trial (the Japan Diabetes Complications Study)," *Diabetologia*, vol. 53, no. 3, pp. 419–428, 2010.

[7] UK Prospective Diabetes Study (UKPDS) Group, "Intensive blood-glucose control with sulphonylureas or insulin compared

with conventional treatment and risk of complications in patients with type 2 diabetes (UKPDS 33)," *The Lancet*, vol. 352, no. 9131, pp. 837–853, 1998.

[8] R. R. Holman, S. K. Paul, M. A. Bethel, D. R. Matthews, and H. A. W. Neil, "10-year follow-up of intensive glucose control in type 2 diabetes," *The New England Journal of Medicine*, vol. 359, no. 15, pp. 1577–1589, 2008.

[9] M. Gall, P. Hougaard, K. Borch-Johnsen, and H. Parving, "Risk factors for development of incipient and overt diabetic nephropathy in patients with non-insulin dependent diabetes mellitus: prospective, observational study," *British Medical Journal*, vol. 314, no. 7083, pp. 783–788, 1997.

[10] M. Ravid, D. Brosh, D. Ravid-Safran, Z. Levy, and R. Rachmani, "Main risk factors for nephropathy in type 2 diabetes mellitus are plasma cholesterol levels, mean blood pressure, and hyperglycemia," *Archives of Internal Medicine*, vol. 158, no. 9, pp. 998–1004, 1998.

[11] R. Retnakaran, C. A. Cull, K. I. Thorne, A. I. Adler, and R. R. Holman, "Risk factors for renal dysfunction in type 2 diabetes: U.K. prospective diabetes study 74," *Diabetes*, vol. 55, no. 6, pp. 1823–1939, 2006.

[12] K. Ogawa, K. Ueda, H. Sasaki et al., "History of obesity as a risk factor for both carotid atherosclerosis and microangiopathy," *Diabetes Research and Clinical Practice*, vol. 66, supplement 1, pp. S165–S168, 2004.

[13] T. Kadowaki, Y. Miyake, R. Hagura et al., "On the pathogenesis of type II diabetes with special reference to diminished insulin response and obesity: a 5–12 year follow-up study of subjects with borderline glucose tolerance," *Tohoku Journal of Experimental Medicine*, vol. 141, pp. 141–146, 1983.

[14] Examination Committee of Criteria for "Obesity Disease" in Japan, Japan Society for the Study of Obesity, "New criteria for "obesity disease" in Japan," *Circulation*, vol. 66, no. 11, pp. 987–992, 2002.

[15] A. Kashiwagi, M. Kasuga, E. Araki et al., "International clinical harmonization of glycated hemoglobin in Japan: from Japan Diabetes Society to National Glycohemoglobin Standardization Program values," *Journal of Diabetes Investigation*, vol. 3, no. 1, pp. 8–10, 2012.

[16] S. Matsuo, E. Imai, M. Horio et al., "Revised equations estimated GFR from serum creatinine," *American Journal of Kidney Diseases*, vol. 53, no. 6, pp. 982–992, 2009.

[17] D. Davis, T. Kern, and L. I. Rand, "Diabetic retinopathy," in *International Textbook of Diabetes Mellitus*, K. G. M. M. Alberti, P. Zimmet, and R. A. DeFronzo, Eds., pp. 1413–1446, John Wiley & Sons, Chichester, UK, 2nd edition, 1997.

[18] T. Ninomiya, V. Perkovic, B. E. de Galan et al., "Albuminuria and kidney function independently predict cardiovascular and renal outcomes in diabetes," *Journal of the American Society of Nephrology*, vol. 20, no. 8, pp. 1813–1821, 2009.

[19] S. Meguro, T. Shigihara, Y. Kabeya, M. Tomita, and Y. Atsumi, "Increased risk of renal deterioration associated with low e-GFR in type 2 diabetes mellitus only in albuminuric subjects," *Internal Medicine*, vol. 48, no. 9, pp. 657–663, 2009.

[20] R. A. Hoefield, P. A. Kalra, P. G. Baker et al., "The use of eGFR and ACR to predict decline in renal function in people with diabetes," *Nephrology Dialysis Transplantation*, vol. 26, no. 3, pp. 887–892, 2011.

[21] H. Yokoyama, S. Kanno, S. Takahashi et al., "Risks for glomerular filtration rate decline in association with progression of albuminuria in type 2 diabetes," *Nephrology Dialysis Transplantation*, vol. 26, no. 9, pp. 2924–2930, 2011.

[22] S. Meguro, M. Tomita, Y. Kabeya et al., "Factors associated with the decline of kidney function differ among eGFR strata in subjects with type 2 diabetes mellitus," *International Journal of Endocrinology*, vol. 2012, Article ID 687867, 6 pages, 2012.

[23] W. R. Ross and J. B. McGill, "Epidemiology of obesity and chronic kidney disease," *Advances in Chronic Kidney Disease*, vol. 13, no. 4, pp. 325–335, 2006.

[24] A. Vivante, E. Golan, D. Tzur et al., "Body mass index in 1.2 million adolescents and risk for end-stage renal disease," *Archives of Internal Medicine*, vol. 172, no. 21, pp. 1644–1650, 2012.

Hindawi Publishing Corporation
International Journal of Endocrinology
Volume 2014, Article ID 302602, 1 page
http://dx.doi.org/10.1155/2014/302602

Hindawi

Erratum

Erratum to "Effect of Telmisartan or Losartan for Treatment of Nonalcoholic Fatty Liver Disease: Fatty Liver Protection Trial by Telmisartan or Losartan Study (FANTASY)"

Takumi Hirata,[1] Kengo Tomita,[1,2] Toshihide Kawai,[1] Hirokazu Yokoyama,[1] Akira Shimada,[1] Masahiro Kikuchi,[1] Hiroshi Hirose,[1] Hirotoshi Ebinuma,[1] Junichiro Irie,[1] Keisuke Ojiro,[1] Yoichi Oikawa,[1] Hidetsugu Saito,[1] Hiroshi Itoh,[1] and Toshifumi Hibi[1]

[1] *Department of Internal Medicine, School of Medicine, Keio University, 35 Shinanomachi, Shinjuku-ku, Tokyo 160-8582, Japan*
[2] *Department of Internal Medicine, National Defense Medical College, 3-2 Namiki, Tokorozawa-Shi, Saitama 359-8513, Japan*

Correspondence should be addressed to Toshihide Kawai; tkawai@a3.keio.jp

Received 5 March 2014; Accepted 16 April 2014; Published 27 April 2014

In the paper, the dosage of telmisartan is incorrect due to a typographical error. Twelve patients, assigned to telmisartan group, received telmisartan at a dose of 40 mg, not 20 mg, once a day. The correct sentences should appear as given below.

(1) "Nineteen hypertensive NAFLD patients with type 2 diabetes were randomly assigned to receive telmisartan at a dose of 40 mg once a day ($n = 12$) or losartan at a dose of 50 mg once a day ($n = 7$) for 12 months" in the "Methods" section of the "Abstract."

(2) "Nineteen hypertensive NAFLD patients with type 2 diabetes were randomly assigned to the telmisartan (T) group (receiving a standard dose of 40 mg once daily, $n = 12$) or the losartan (L) group (receiving a standard dose of 50 mg once daily, $n = 7$)" in Section 2.2.

Am J Physiol Gastrointest Liver Physiol 304: G700–G707, 2013.
First published February 28, 2013; doi:10.1152/ajpgi.00318.2012.

CCR2 knockout exacerbates cerulein-induced chronic pancreatitis with hyperglycemia via decreased GLP-1 receptor expression and insulin secretion

Yuji Nakamura,[1] Takanori Kanai,[1] Keita Saeki,[1] Miho Takabe,[1] Junichiro Irie,[2] Jun Miyoshi,[1] Yohei Mikami,[1] Toshiaki Teratani,[1] Takahiro Suzuki,[1] Naoteru Miyata,[1] Tadakazu Hisamatsu,[1] Nobuhiro Nakamoto,[1] Yoshiyuki Yamagishi,[1] Hajime Higuchi,[1] Hirotoshi Ebinuma,[1] Shigenari Hozawa,[1] Hidetsugu Saito,[1] Hiroshi Itoh,[2] and Toshifumi Hibi[1]

Divisions of [1]Gastroenterology and Hepatology and [2]Endocrinology, Department of Internal Medicine, Keio University School of Medicine, Tokyo, Japan

Submitted 31 July 2012; accepted in final form 13 February 2013

Nakamura Y, Kanai T, Saeki K, Takabe M, Irie J, Miyoshi J, Mikami Y, Teratani T, Suzuki T, Miyata N, Hisamatsu T, Nakamoto N, Yamagishi Y, Higuchi H, Ebinuma H, Hozawa S, Saito H, Itoh H, Hibi T. CCR2 knockout exacerbates cerulein-induced chronic pancreatitis with hyperglycemia via decreased GLP-1 receptor expression and insulin secretion. *Am J Physiol Gastrointest Liver Physiol* 304: G700–G707, 2013. First published February 28, 2013; doi:10.1152/ajpgi.00318.2012.—Glucagon-like peptide-1 (GLP-1) promotes insulin release; however, the relationship between the GLP-1 signal and chronic pancreatitis is not well understood. Here we focus on chemokine (C-C motif) ligand 2 (CCL2) and its receptor (CCR2) axis, which regulates various immune cells, including macrophages, to clarify the mechanism of GLP-1-mediated insulin secretion in chronic pancreatitis in mice. One and multiple series of repetitive cerulein administrations were used to induce acute and chronic cerulein pancreatitis, respectively. Acute cerulein-administered CCR2-knockout (KO) mice showed suppressed infiltration of $CD11b^{+}Gr\text{-}1^{low}$ macrophages and pancreatic inflammation and significantly upregulated insulin secretion compared with paired wild-type (WT) mice. However, chronic cerulein-administered CCR2-KO mice showed significantly increased infiltration of $CD11b^{+}/Gr\text{-}1^{-}$ and $CD11b^{+}/Gr\text{-}1^{high}$ cells, but not $CD11b^{+}/Gr\text{-}1^{low}$ cells, in pancreas with severe inflammation and significantly decreased insulin secretion compared with their WT counterparts. Furthermore, although serum GLP-1 levels in chronic cerulein-administered WT and CCR2-KO mice were comparably upregulated after cerulein administrations, GLP-1 receptor levels in pancreases of chronic cerulein-administered CCR2-KO mice were significantly lower than in paired WT mice. Nevertheless, a significantly higher hyperglycemia level in chronic cerulein-administered CCR2-KO mice was markedly restored by treatment with a GLP-1 analog to a level comparable to the paired WT mice. Collectively, the CCR2/CCL2 axis-mediated $CD11b^{+}$-cell migration to the pancreas is critically involved in chronic pancreatitis-mediated hyperglycemia through the modulation of GLP-1 receptor expression and insulin secretion.

cerulein; pancreatitis; macrophage; glucose tolerance; islet cell

IN THE YEAR 2000, more than 171 million people worldwide were reported to have diabetes; it is estimated that this number will almost double by 2030 (23). Diabetes is a serious metabolic disorder that causes hyperglycemia as a result of poor insulin production and insulin resistance. Clinical evidence shows that diabetes occurs in the late phase of chronic pancreatitis. Numerous clinical cases of chronic pancreatitis and insulin therapy have been studied; however, the relationship between chronic pancreatitis and insulin secretion is still unknown.

Therapies for chronic pancreatitis include changing patients' alcohol habits and prescribing drugs of digestive enzymes and/or analgesic drugs, which are usually effective to control the symptoms. Because chronic pancreatitis is rarely treated with surgery, specimens of pancreatic β-cells from patients with chronic pancreatitis are difficult to obtain; histological investigation of such tissue is consequently challenging. Therefore, animal models are often used to investigate the relationship between insulin secretion and chronic pancreatitis. Cerulein-induced pancreatitis is a standard model for investigating acute pancreatitis (12) and chronic pancreatitis (24). However, the mechanism of insulin secretion in the chronic model of the disease is unclear.

Infiltration of mononuclear cells is a hallmark of pathogenesis of various immune diseases. Among them, macrophages play a key role in innate immunity for the maintenance of homeostasis, for example inflammation dampening via the production of anti-inflammatory cytokines such as IL-10 and TGF-β, debris scavenging, angiogenesis, and wound healing (9, 11). Chemokine (C-C motif) ligand 2 (CCL2) is a small cytokine of the CC chemokine family, and its receptor (CCR2) plays an important role in the recruitment of monocytes, memory T cells, and peritoneal macrophages in inflammatory tissues (1, 19, 22). Recently we showed that CCL2-deficient mice are resistant to acute cerulein pancreatitis by affecting the migration of pathological TNF-α-producing $CD11b^{high}/CD11c^{-}/Gr\text{-}1^{low}$ macrophages (16). However, no studies on the role of the CCR2/CCL2 axis and its involvement in insulin secretion in chronic pancreatitis have been reported to date.

Glucagon-like peptide-1 (GLP-1), secreted from intestinal L cells, is associated with increased intracellular cyclic AMP, leading to insulin release from β-cells during hyperglycemia and suppression of inappropriate glucagon secretion from α-cells. Consistent with this mechanism, a long-acting GLP-1 analog, liraglutide, has been developed for the treatment of type 2 diabetes (14). However, the relationship between GLP-1 and diabetes with chronic pancreatitis has not been clarified.

The aims of this study were to clarify the role of the CCR2/CCL2 axis in the pathogenesis of chronic cerulein pancreatitis and to examine the mechanisms underlying insulin secretion and GLP-1 signals in chronic pancreatitis.

MATERIALS AND METHODS

Animals. Breeding pairs of CCR2-deficient mice (knockout) (CCR2-KO) on a C57BL/6J background (Jackson Laboratory, Bar

Address for reprint requests and other correspondence: Y. Nakamura, Div. of Gastroenterology and Hepatology, Dept. of Internal Medicine, Keio Univ. School of Medicine, 35 Shinanomachi, Shinjuku, Tokyo 160-8582, Japan (e-mail: yujinaka@a5.keio.jp).

Harbor, ME) and wild-type (WT) C57BL/6J mice (Charles River Laboratories Japan, Tokyo, Japan) were used. All mice were maintained and bred at the animal facilities at Keio University, Japan, and all experiments were approved by and performed according to the guidelines of the Experimental Animal Committee of Keio University, School of Medicine.

Mouse models of acute and chronic cerulein pancreatitis. Acute cerulein pancreatitis was induced in 8-wk-old male mice with seven hourly intraperitoneal injections of cerulein (American Peptide, Sunnyvale, CA), at a dose of 50 μg/kg. Chronic cerulein pancreatitis was induced by six hourly intraperitoneal injections of cerulein, at a dose of 50 μg/kg, given twice per week for 10 wk (25). Control animals were injected with the same volume of physiological saline. Mice were euthanized with an overdose of pentobarbital. Blood and pancreatic tissues were collected 1 h after the final cerulein injection for acute pancreatitis and at 8:00 in the morning 1 wk after the final cerulein injection for chronic pancreatitis.

Histological analyses, including interstitial space, necrosis, islet cell, and fibrotic space using hematoxylin and eosin (HE) stain and Masson-Trichrome stain, were quantified using a LuminaVision analysis system (Mitani, Fukui, Japan) (10, 13).

Blood examination. Concentrations of serum amylase (AMY) and lipase (LIP) were measured by a commercial laboratory (SRL, Tokyo, Japan). Plasma glucose was measured with a Onetouch UltraVue meter (Johnson & Johnson, New Brunswick, NJ), serum insulin with an insulin measuring kit (Morinaga Institute of Biological Science, Kanagawa, Japan), and plasma GLP-1(7–36) and GLP-1(9–36) with an enzyme immunoassay kit (Yanaihara Laboratory, Shizuoka, Japan), according to manufacturers' instructions.

Immunohistochemistry. Pancreatic tissue fixed with paraffin was deparaffinized in xylene, hydrated with ethanol, and finally rinsed in PBS. Anti-insulin antibody (Dako, Glostrup, Denmark) and GLP-1R antibody (Abcam, Cambridge, UK) were used as primary antibodies and were incubated with a mixture of two fluorescence-conjugated secondary antibodies [FITC-conjugated goat anti-guinea pig antibody for insulin (Abcam) and Alexa-568-conjugated goat anti-rabbit antibody for GLP-1R (Invitrogen, Carlsbad, CA)] in PBS for 30 min at room temperature.

Western blotting. Pancreatic tissues taken from the mice after euthanasia were immediately frozen in liquid nitrogen and stored at −80°C. The tissues were homogenized with RIPA buffer (Thermo Scientific, Rockford, IL) containing protease inhibitors (Thermo Scientific). After being centrifuged for 15 min at 4°C at 14,000 revolution/min, the supernatant was transferred to new tubes, and protein concentrations were determined with a BCA protein assay kit (Pierce, Rockford, IL). Samples were run on NuPAGE 4–12% Bis-Tris gels (Invitrogen) and transferred to PVDF membranes (GE Healthcare, Buckinghamshire, UK). The membranes were incubated with primary antibodies against GLP-1R, insulin, and β-actin (Santa Cruz Biotechnology, Santa Cruz, CA).

Flow cytometry analysis. Fresh pancreatic tissue was minced and digested with 3 mg/ml collagenase A (Roche, Mannheim, Germany) for 15 min at 37°C. The digest was filtered through a 40-μm cell strainer and washed with Hank's balanced salt solution containing 1.5% FCS, as described previously (16). Viability was ascertained using with 7-AAD and annexin V (BD Pharmingen, Franklin Lakes, NJ) double staining; specimens with ≥80% living cells were selected for examination. Isolated cells were incubated with anti-CD16/CD32 antibody (BD Pharmingen) to prevent nonspecific antibody binding. Surface antigens were stained with CD11b-phycoerythrin-Cy7 and Ly6C-allophycocyanin-Cy7 (Gr-1, clone: RB6–8C5; BD Pharmingen). Flow cytometry was performed on a FACSCanto II/TM (BD

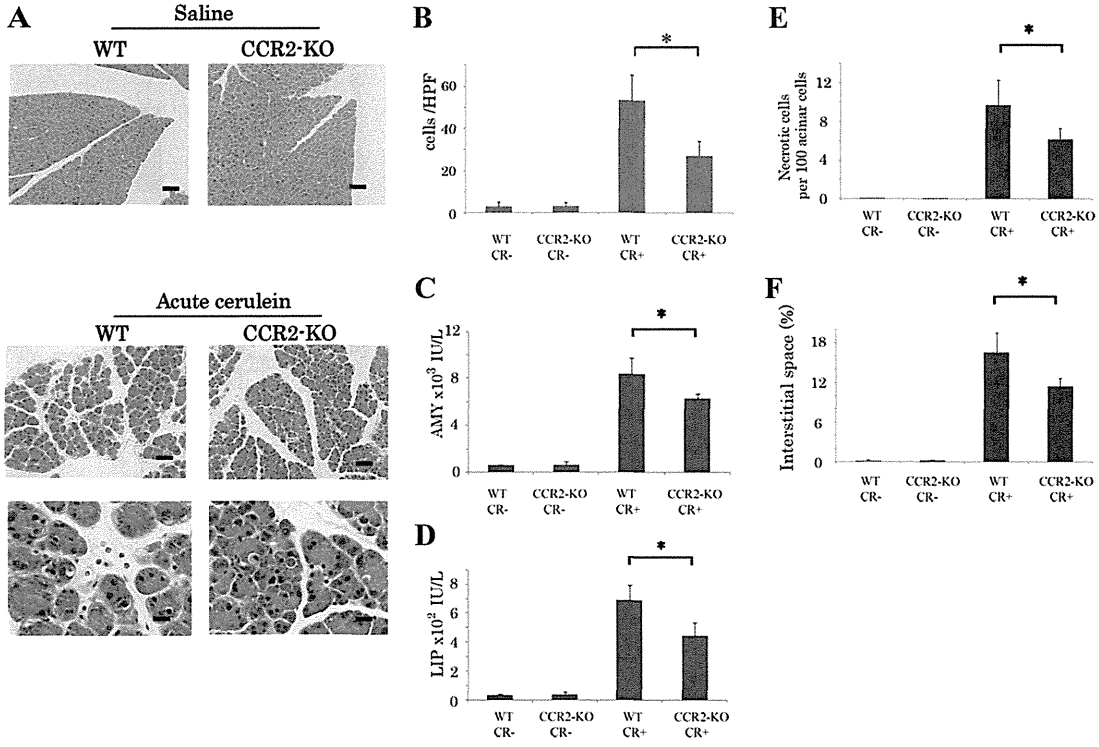

Fig. 1. Mouse model of acute cerulein pancreatitis. *A*: micrographs of pancreatic tissues with hematoxylin and eosin (HE) staining for acute cerulein pancreatitis (scale bar = 100 μm, *top* and *middle*; scale bar = 10 μm, *bottom*). Wild-type (WT) and chemokine (C-C motif) ligand 2 (CCL2) receptor knockout (CCR2-KO) mice were given 7 hourly cerulein injections (CR+) or saline injections (CR-). *B*: total number of inflammatory cells in each high-power field (HPF). Levels of serum amylase (AMY) and lipase (LIP) were measured in blood taken from mice 1 h after the final cerulein injection. *C*: serum AMY levels. *D*: serum LIP levels. *E*: total number of necrotic cells per 100 acinar cells. *F*: percentage of interstitial space in each HPF. *B*, *E*, and *F* evaluations were averaged by counting the numbers in each pancreas in 10 fields. $N = 5$. $^*P < 0.05$.

Biosciences, San Jose, CA). All data were reanalyzed with FlowJo Version 7.2.5 software (TreeStar, Ashland, OR).

Glucose tolerance test and insulin sensitivity. Glucose tolerance test (GTT) was performed to measure changes in blood glucose concentrations after an intravenous injection of 20% glucose at 2 g/kg. Insulin sensitivity was measured by examining the changes in blood glucose levels after an intravenous injection of regular insulin Novolin R (Novo Nordisk Pharma, Bagsvaerd, Denmark), at a dosage of 0.75 U/kg. GTT was performed on WT and CCR2-KO mice with chronic pancreatitis treated with and without the GLP analog, liraglutide (Novo Nordisk Pharma). For 3 days before the GTT, liraglutide was injected intraperitoneally twice each day at dosages of 100 μg/kg body wt on the first day, 200 μg/kg on the second day, and 300 μg/kg on the final day.

Quantitative RT-PCR analysis with isolated islet cells. Islet RNA was extracted with Trizol (Invitrogen) from isolated mouse islet cells, as previously described (8) using collagenase-p (Roche, Basel, Switzerland). Reverse transcription and quantitation of mRNA expression were performed as previously described (20) using the SYBR Premix Ex Taq (Perfect Real Time) kit in a Thermal Cycler Dice Real Time system (TaKaRa Biologicals, Ohtsu, Shiga, Japan).

Statistical analysis. All data are expressed as means ± SD. The two-tailed nonparametric test (unpaired *t*-test) was used for statistical analysis. $P < 0.05$ were considered statistically significant.

RESULTS

CCR2-KO mice were resistant to acute cerulein pancreatitis. Acute cerulein pancreatitis in WT and CCR2-KO mice was analyzed with HE staining of pancreatic tissues, and serum AMY and LIP levels were measured. We confirmed that both WT and CCR2-KO mice were healthy until they were 40 wk old (data not shown). Saline-administered WT and CCR2-KO mice showed no pancreas abnormalities. In contrast, cerulein-administered WT mice developed acute pancreatitis with edema and infiltration of inflammatory cells into the pancreas; however, the severity in cerulein-administered CCR2-KO mice was markedly reduced (Fig. 1*A*). Consistently, absolute numbers of inflammatory cells (Fig. 1*B*), serum AMY (Fig. 1*C*), serum LIP (Fig. 1*D*), necrotic cells (Fig. 1*E*), and interstitial space (Fig. 1*F*) in cerulein-administered CCR2-KO mice were

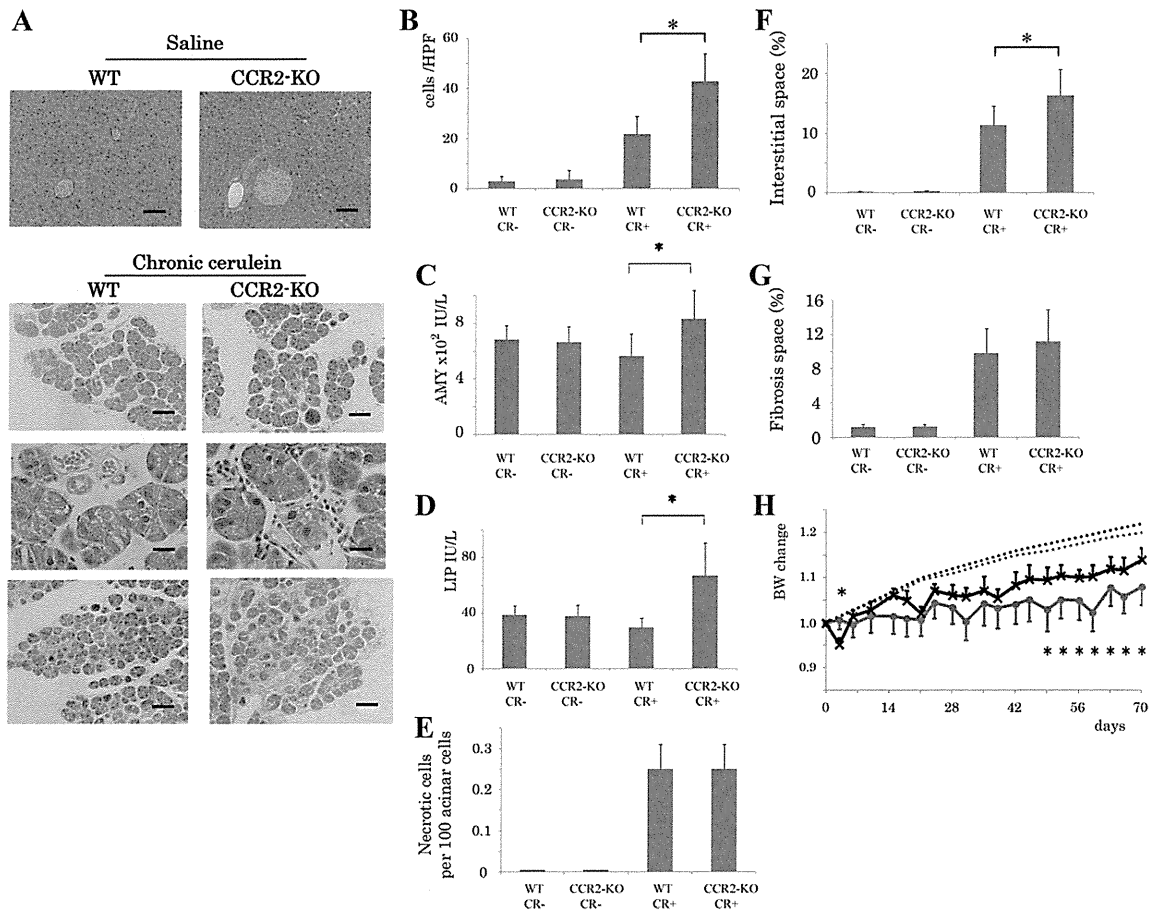

Fig. 2. Mouse model of chronic cerulein pancreatitis. *A*: micrographs of pancreatic tissues with HE staining for chronic cerulein pancreatitis (scale bar = 100 μm, *top* and *top, middle*; scale bar = 10 μm, *bottom, middle*), and micrographs of pancreas tissues with Masson trichrome staining for chronic cerulein pancreatitis (scale bar = 100 μm, *bottom*). WT and CCR2-KO mice were treated with cerulein injections or saline injections for 10 wk. *B*: total number of inflammatory cells in each HPF. Levels of serum AMY and LIP were measured in blood taken from mice 1 wk after the final cerulein injection. *C*: serum AMY levels. *D*: serum LIP levels. *E*: total number of necrotic cells per 100 acinar cells. *F*: percentage of interstitial space in each HPF. *G*: percentage of fibrosis space in each HPF. *B*, *E*, *F*, and *G* evaluations were averaged by counting the numbers in each pancreas in 10 fields. $N = 5$. $^*P < 0.05$. *H*: changes in body weight (BW) of WT and CCR2-KO mice over the course of chronic cerulein pancreatitis. Changes were calculated from body weights measured before and after pancreatitis onset. Red line and circles, CCR2-KO CR^+ mice; black line and crosses, WT CR^+ mice; red dashed line, CCR2-KO CR^- mice; black dashed line, WT CR^- mice. $N = 5$. $^*P < 0.05$ compared with CCR2-KO CR^+ mice from WT CR^+ mice.

significantly less than in cerulein-administered WT mice, whereas no differences were observed between the two types in the paired saline-administered mice.

CCR2-KO mice were sensitive to chronic cerulein pancreatitis. In contrast to the saline-administered mice, long-term administration of cerulein for the chronic model induced severe edema, infiltration of inflammatory cells, and fibrosis (Fig. 2*A*). Surprisingly, however, contrary to the results observed in acute cerulein pancreatitis, cerulein-administered CCR2-KO mice developed severe pancreatitis compared with the WT mice (Fig. 2*A*). The absolute numbers of inflammatory cells (Fig. 2*B*), the serum AMY (Fig. 2*C*) and LIP (Fig. 2*D*), and interstitial space (Fig. 2*F*) in cerulein-administered CCR2-KO mice were significantly higher than in cerulein-administered WT mice, whereas no differences were observed between the two mouse types in the paired saline-administered mice. Necrotic cells and fibrosis space did not significantly differ between cerulein-administered WT and CCR2-KO mice (Fig. 2, *E* and *G*). As with the acute model (Fig. 1), the body weight of cerulein-administered WT mice decreased after the first sequential cerulein injection, whereas their cerulein-administered CCR2-KO counterparts maintained their body weight (Fig. 2*E*). However, 1 wk after the onset of chronic cerulein pancreatitis, the body weight of cerulein-administered WT mice started to increase more rapidly than that of the cerulein-administered CCR2-KO mice and, at 7 wk after the first injection, was significantly higher than that of the cerulein-administered CCR2-KO mice, which had more severe pancreatitis. The body weight of WT mice and CCR2-KO mice that received saline injections for 10 wk did not differ.

$CD11b^+/Gr\text{-}1^-$ and $CD11b^+/Gr\text{-}1^{high}$ macrophages markedly accumulated in CCR2-KO mice receiving long-term cerulein. Phenotypes of inflammatory cells in the pancreas were analyzed with flow cytometry. Consistent with our previous results (16), in the acute cerulein pancreatitis model, the absolute number of $CD11b^+/Gr\text{-}1^{low}$ cells in the pancreas of cerulein-administered WT mice was significantly higher than in the cerulein-administered CCR2-KO mice (Fig. 3, *C* and *D*). The saline-administered WT and CCR2-KO mice showed no significant differences in inflammatory cells (Fig. 3, *A* and *B*). In the chronic cerulein pancreatitis model, $CD11b^+/Gr\text{-}1^{low}$ macrophages disappeared; however, the absolute cell numbers of $CD11b^+/Gr\text{-}1^-$ and $CD11b^+/Gr\text{-}1^{high}$ macrophages in pancreases of cerulein-administered CCR2-KO mice were significantly higher than in cerulein-administered WT mice (Fig. 3, *E* and *F*).

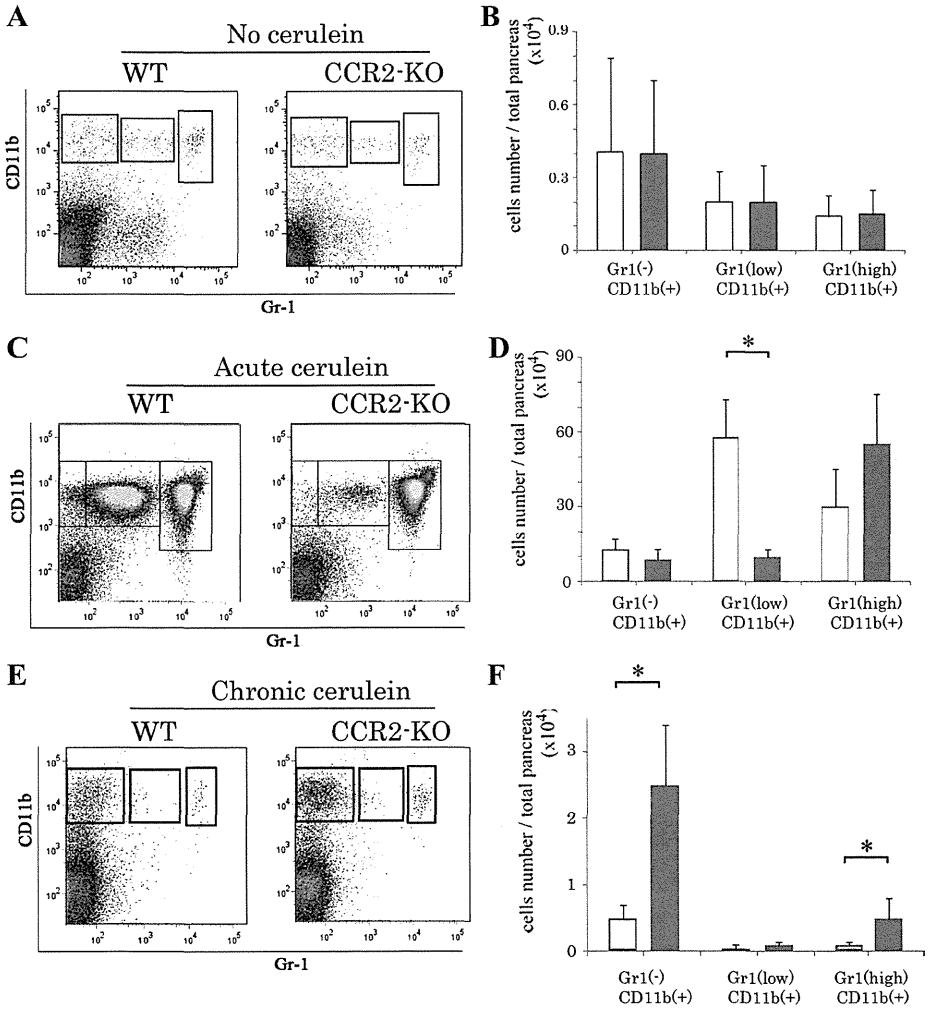

Fig. 3. Analysis of inflammatory cell phenotypes in acute and chronic cerulein pancreatitis. Flow cytometry shows $CD11b^+$ and $Gr\text{-}1^+$ cells among isolated cells from the pancreas after collagenase digestion. Cells were grouped as $Gr1^-/CD11b^+$, $Gr1^{low}/CD11b^+$, and $Gr1^{high}/CD11b^+$. Cell numbers in each group were determined by flow cytometry. *A* and *B*: flow cytometry and cell numbers without cerulein pancreatitis. *C* and *D*: flow cytometry and cell numbers in acute cerulein pancreatitis. *E* and *F*: flow cytometry and cell numbers in chronic cerulein pancreatitis. Open bar, WT mice; shaded bar, CCR2-KO mice. Flow cytometry is representative of 5 independent experiments; $N = 5$. $^*P < 0.05$.

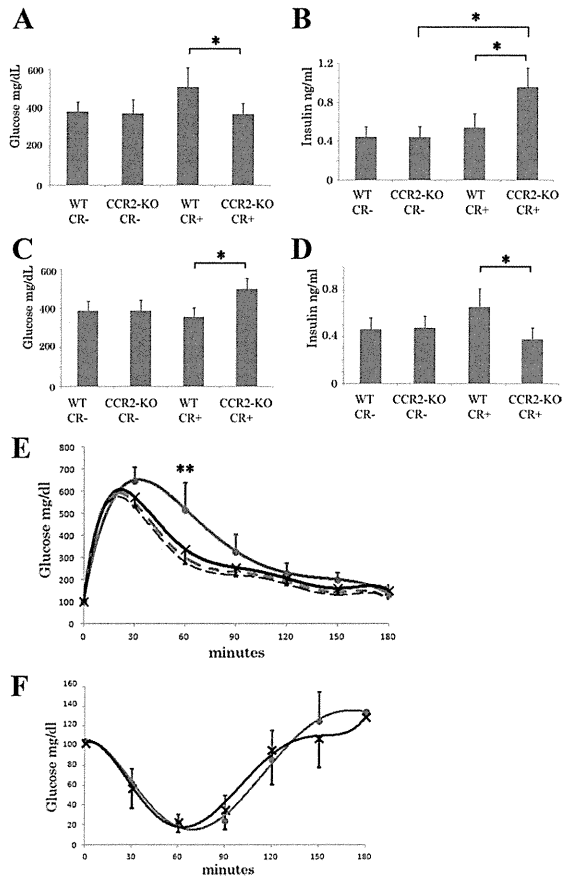

Fig. 4. Plasma glucose and serum insulin concentrations. Blood samples were taken 1 h after the final cerulein injection in acute pancreatitis and at 8:00 in the morning 1 wk after the final cerulein injection in chronic pancreatitis; mice had unrestricted access to food and water. Mice were treated with cerulein or with saline. *A* and *B*: plasma glucose concentration and serum insulin concentration in acute cerulein pancreatitis. *C* and *D*: plasma glucose concentration and serum insulin concentration in chronic cerulein pancreatitis. *E*: glucose tolerance test (GTT) in chronic cerulein pancreatitis measured changes in blood glucose levels after intravenous injection of 20% glucose 2 g/kg body wt. *F*: for insulin sensitivity, changes in blood glucose levels were measured after intravenous injection of regular insulin at a dose of 0.75 U/kg body wt. Red line and circles, CCR2-KO CR+ mice; black line and crosses, WT CR+ mice; red dashed line, CCR2-KO CR$^-$ mice; black dashed line, WT CR$^-$ mice. $N = 5$. $^*P < 0.05$. $^{**}P < 0.05$ compared with CCR2-KO CR$^+$ and WT CR$^+$ mice.

CCR2-KO mice that received long-term cerulein developed severe hyperglycemia with less insulin production. Concentrations of blood glucose and serum insulin were measured in mice that had in acute and chronic cerulein pancreatitis and given unrestricted access to food and water. In the acute pancreatitis model, cerulein-administered CCR2-KO mice showed lower blood glucose than did paired WT mice, but the saline-administered WT and CCR2-KO mice did not differ (Fig. 4*A*). Consistently, serum insulin concentrations in cerulein-administered CCR2-KO mice were significantly higher than in their paired WT counterparts, but there was no difference between the saline-administered groups of mice (Fig. 4*B*). In the chronic pancreatitis model, results were the reverse of those in the acute pancreatitis model; chronic cerulein-administered CCR2-KO mice showed higher blood glucose (Fig. 4*C*) and less insulin secretion (Fig. 4*D*) compared with the chronic cerulein-administered WT mice.

We next conducted GTTs to confirm glucose intolerance in the chronic pancreatitis models. The GTT showed greater glucose levels in the chronic cerulein-administered CCR2-KO mice than in the chronic cerulein-administered WT mice (Fig. 4*E*), but no differences in GTT between WT and CCR2-KO mice without cerulein pancreatitis were observed. On the other hand, insulin sensitivity in cerulein-administered mice was not different in the two types of mice (Fig. 4*F*), indicating that poor insulin secretion is the major cause of glucose intolerance in chronic cerulein-administered CCR2-KO mice.

Islet number and size did not decrease in mice receiving long-term cerulein. Because CCR2-KO mice had more severe pancreatitis than WT mice, the number and size of islets in chronic cerulein pancreatitis were counted in each mouse. The number of islets from mice with cerulein-induced chronic pancreatitis was greater than that from paired mice without cerulein (Fig. 5*A*), but the difference between WT and CCR2-KO mice was not significant. The sizes of islets in mice with cerulein-induced chronic pancreatitis were not different between WT and CCR2-KO mice with and without cerulein-induced chronic pancreatitis (Fig. 5*B*).

GLP-1 receptor expression was downmodulated in CCR2-KO mice receiving long-term cerulein. One mechanism of insulin secretion from pancreatic β-cells involves the GLP-1 signal (5). Therefore, serum GLP-1 and GLP-1 receptor in the pancreas were measured. To exclude differences in food intake among the mice, tissues and blood samples were taken following overnight fasting. GLP-1 levels in chronic cerulein-administered WT and CCR2-KO mice were found to be greater than in the paired saline-administered mice (Fig. 6*A*). However, there were no differences in GLP-1 levels between WT and CCR2-KO mice, irrespective of saline or cerulein administration (Fig. 6*A*). In contrast, GLP-1R expression in the pancreas of chronic cerulein-administered WT and CCR2-KO mice was significantly lower than in the paired saline-administered mice, but the decrease was greater in cerulein-administered CCR2-KO mice, resulting in a significant difference between cerulein-administered WT and CCR2-KO mice, whereas the insulin levels were not different between these groups (Fig. 6, *B* and *C*). The immunohistochemistry results for insulin and GLP-1R in pancreatic tissues also showed lower GLP-1R expression in cerulein-administered CCR2-KO mice than in their cerulein-administered WT counterparts, whereas insulin levels were

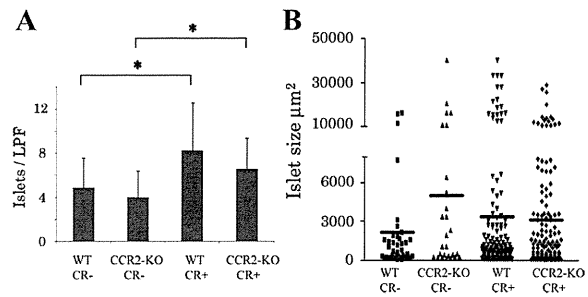

Fig. 5. Numbers and sizes of islet cells in chronic cerulein pancreatitis. *A*: total number of islet cells was counted in each low-power field (LPF). *B*: sizes of islet cells were measured in each LPF. Averages were calculated by analyzing each pancreas in 10 fields. $N = 5$. $^*P < 0.05$.

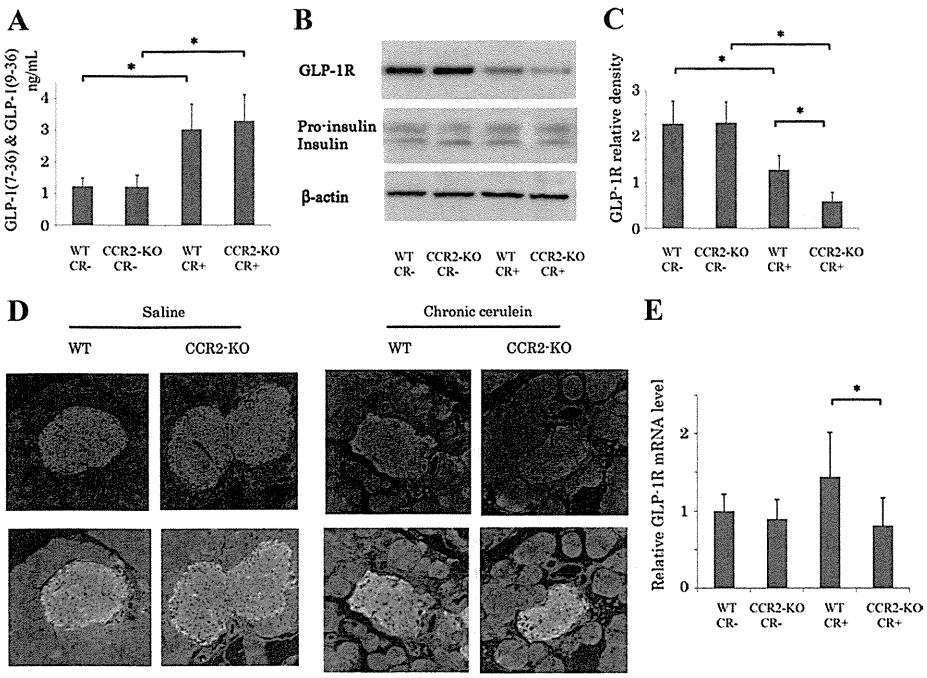

Fig. 6. Glucagon-like peptide 1 receptor (GLP-1R) levels in pancreatic tissue with chronic cerulein pancreatitis. *A*: plasma GLP-1 levels in WT and CCR2-KO mice with chronic cerulein pancreatitis. *B*: Western blots of GLP-1R and insulin from pancreatic tissue with chronic cerulein pancreatitis. *C*: relative GLP-1R quantification. Blots were reprobed for β-actin used as a loading control, and the bands were quantified by densitometry. Mice were treated with cerulein injections or saline injections for 10 wk. Tissue and blood samples were taken from mice after overnight fasting. Blots were representative of 5 independent experiments. *D*: immunohistochemistry for insulin and GLP-1R in chronic cerulein pancreatitis. Shown are micrographs of pancreatic tissues (×400) with insulin antibody with FITC (green), and GLP-1R antibody with Alexa-568 (red). *E*: quantization of mRNA expression for *GLP-1R* in isolated islet cells. The amount of mRNA was normalized to 18S mRNA. $N = 5$. $^*P < 0.05$.

comparable in both groups (Fig. 6*D*). Because islet cells are only 1–2% of total pancreatic cells, RT-PCR for *GLP-1R* in isolated islet cells from each mouse was analyzed; *GLP-1R* mRNA expression was lower in CCR2-KO with chronic cerulein-administered mice than WT with chronic cerulein-administered mice, but no difference was seen between WT and CCR2-KO without cerulein pancreatitis (Fig. 6*E*).

GLP-1 analog treatment rescued impaired glucose tolerance in chronic cerulein-administered mice. Last, we examined the effects of the GLP-1 analog, liraglutide, on mice with chronic cerulein pancreatitis. To evaluate pancreatitis with liraglutide treatment, pancreas and blood from WT mice were analyzed. The severity of pancreatitis was not different, and inflammatory cell infiltration of pancreas was higher, but not significantly higher, in mice with liraglutide treatment (Table 1). Fluorescence-activated cell sorting analysis showed cell numbers increasing after liraglutide treatment, but flow cytometry showed no specific pattern for CD11b and Gr-1 (Fig. 7, *A* and *B*). Flow cytometry data of chronic pancreatitis without liraglutide treatment was the same as that of chronic pancreatitis as shown in Fig. 3, *E* and *F*. Surprisingly, our data showed that liraglutide treatment rescued the impaired glucose tolerance of the cerulein-administered CCR2-KO mice (Fig. 7*C*).

Table 1. *Chronic cerulein pancreatitis and liraglutide treatment*

	CP	CP + Liraglutide	*P* Value
AMY, IU/ml	560 ± 73	610 ± 82	N.S.
LIP, IU/ml	32 ± 5.6	33 ± 7.1	N.S.
Cell Infiltration Cells/HPF	20 ± 9	30 ± 14	N.S.
Necrotic Cells per 100 Acinar Cells	0.25 ± 0.05	0.26 ± 0.05	N.S.
Interstitial Space, %	11 ± 4.9	10 ± 4.5	N.S.
Fibrosis Space, %	9.9 ± 2.9	9.6 ± 3.4	N.S.

Values are means ± SD. Wild-type (WT) mice were treated with cerulein injections (CR^+) for 10 wk, and then treated with the glucagon-like peptide 1 (GLP-1) analog, liraglutide, for 3 days. Levels of serum amylase (AMY) and lipase (LIP) were measured in blood taken from mice on the day after the final liraglutide injection. Total number of inflammatory cells in each high-power field (HPF), total number of necrotic cells per 100 acinar cells, percentage of interstitial space in each HPF, and percentage of fibrosis space in each HPF, were averaged by analyzing each pancreas in 10 fields. $N = 5$. CP, cerulein pancreatitis; N.S.; not significant.

DISCUSSION

Although chronic pancreatitis is closely related to insulin insufficiency and diabetes mellitus (2), the molecular relationship between insulin secretion and chronic pancreatitis is unclear (17). This study demonstrates that CCR2-KO mice receiving long-term cerulein develop more severe chronic pancreatitis via *1*) downmodulation of GLP-1R expression, *2*) decrease in insulin release, and *3*) hyperglycemia. It also provides the first evidence of a protective role for the CCR2/CCL2 axis against diabetes.

The CCR2/CCL2 axis plays a pivotal role in the pathogenesis of many immune diseases characterized by mononuclear cell infiltration, including chronic pancreatitis (16). First, our present study showed that CCR2-KO mice develop less severe acute cerulein pancreatitis with decreased accumulation of $CD11b^+/Gr\text{-}1^{low}$ macrophages. This was not surprising, as we previously showed that CCL2-KO mice developed less severe pancreatitis with less infiltration of TNF-α-expressing $CD11b^+/Gr\text{-}1^{low}/F4/80^+$ macrophages into the pancreas. Taken together, we conclude that $CCR2^+$ macrophages are involved in the pathogenesis of pancreas tissue damage, at least in the acute phase of pancreatitis. However, it was very surprising that, compared with WT mice, CCR2-KO mice reproducibly developed more severe chronic cerulein pancreatitis with accumulation of $CD11b^+/Gr\text{-}1^-$ and $CD11b^+/Gr\text{-}1^{high}$, but not $CD11b^+/Gr\text{-}1^{low}$, macrophages. Together with the histological findings on the long-term cerulein-administered CCR2-KO

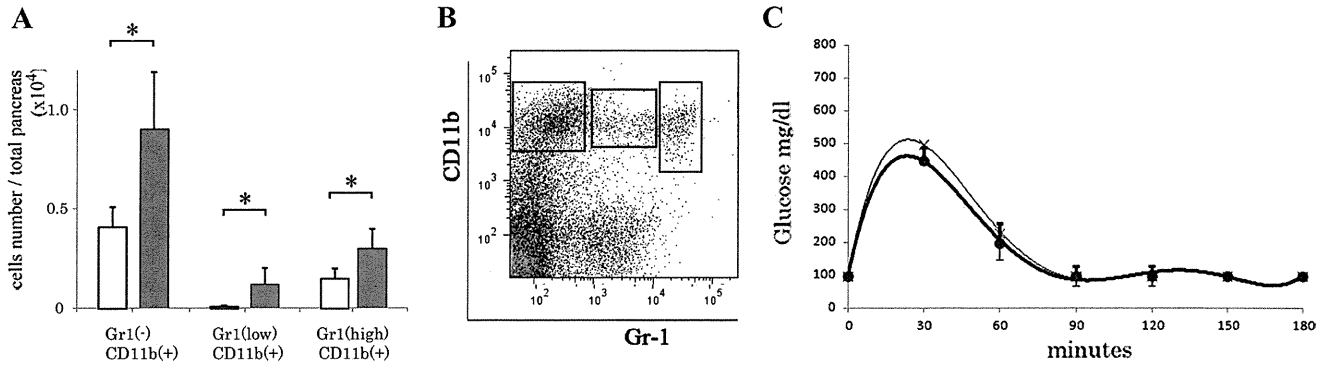

Fig. 7. WT and CCR2-KO mice were treated with cerulein injections or saline injections for 10 wk, and then with the GLP-1 analog, liraglutide, for 3 days. *A*: cell numbers calculated by flow cytometry in WT mice with chronic cerulein pancreatitis with or without liraglutide. Open bar, without liraglutide (similar to Fig 3*F*); shaded bar, with liraglutide. Flow cytometry is representative of 5 independent experiments; $N = 5$. $^*P < 0.05$. *B*: flow cytometry in WT mice with chronic cerulein pancreatitis after liraglutide treatment. *C*: GTT results after 3 days of treatment with GLP-1 analog. Changes in blood glucose levels were measured after intravenous injection of 20% glucose 2 g/kg body wt. Bold line and circles, CCR2-KO mice; thin line and crosses, WT mice.

mice, it seems that $CCR2^+$ cells (yet unidentified) emerge at the late phase of pancreatitis to mediate tissue repair of chronic pancreatitis, but lack of these cells may allow the accumulation of other immune components, including $CD11b^+/Gr\text{-}1^-$ and $CD11b^+/Gr\text{-}1^{high}$ macrophages. Further studies are warranted to clarify the protective role of $CCR2^+$ monocytes in chronic pancreatitis.

A previous study showed that insulin secretion in rats with chronic pancreatitis was significantly lower than in controls (4). We found a consistent inverse relationship between levels of chronic pancreatic damage and insulin secretion, as insulin secretion was markedly impaired in the chronic cerulein-administered CCR2-KO mice but well-preserved in acute cerulein-administered CCR2-KO mice. This also suggests that a CCR2-dependent tissue repair system arises after acute inflammation to maintain insulin secretion. Presently, the mechanism of decreased insulin secretion in chronic pancreatitis is unclear. We confirmed that plasma GLP-1 levels in chronic pancreatitis increased to similar levels in both WT and CCR2-KO mice, as reported previously (6). However, this is the first report to show a significant decrease in GLP-1R expression in chronic cerulein-administered CCR2-KO mice compared with paired WT mice. Therefore, we conclude that, in chronic cerulein-administered CCR2-KO mice, which lack such a CCR2-dependent tissue repair system at the late phase of inflammation, other mechanisms induce the downmodulation of GLP-1R expression.

Last, the clinical relevance of this study should be debated. In this study, we also showed that treatment with a GLP-1 analog diminished the differences in GTT between chronic cerulein-administered WT and CCR2-KO mice, indicating that GLP-1 treatment is appropriate for patients with diabetes secondary to chronic pancreatitis, who clinically appear to have impaired insulin secretion (21). Moreover, the finding that GLP-1 analog treatment improves GTT in a mouse model of chronic pancreatitis is new. Therefore, we propose that GLP-1 analog is a potential candidate to treat diabetes induced in chronic pancreatitis. Although GLP-1 analog treatment has been thought to have adverse effects on the pancreas, such as acute pancreatitis and pancreatic neoplasm, recent studies have reported no associated risk of pancreatic diseases (3, 15). Furthermore, recent studies reported that GLP-1 induces macrophage polarization toward the M2 phenotype (18) and has other anti-inflammatory effects (7). As our data of GLP-1 analog injection over 3 days showed no protective or adverse roles for pancreatitis, longer treatment with a GLP-1 analog should be necessary to clarify any effects for chronic pancreatitis.

ACKNOWLEDGMENTS

We thank Mina Kitazume for excellent assistance with animal care.

GRANTS

This work was supported by Grants-in-Aid for Scientific Research from the Japanese Ministry of Education (to T. Kanai, no. 21390233, and to T. Hibi, no. 21249048).

DISCLOSURES

No conflicts of interest, financial or otherwise, are declared by the authors.

AUTHOR CONTRIBUTIONS

Author contributions: Y.N., T.K., and J.I. conception and design of research; Y.N., K.S., and T.M. performed experiments; Y.N., T.K., and J.I. analyzed data; Y.N., T.K., K.S., J.I., J.M., Y.M., T.T., T.S., N.M., T. Hisamatsu, N.N., Y.Y., H.H., H.E., S.H., H.S., and H.I. interpreted results of experiments; Y.N. and T.K. prepared figures; Y.N. drafted manuscript; Y.N., T.K., and J.I. edited and revised manuscript; Y.N., T.K., and T. Hibi approved final version of manuscript.

REFERENCES

1. **Boring L, Gosling J, Chensue SW, Kunkel SL, Farese RV Jr, Broxmeyer HE, Charo IF.** Impaired monocyte migration and reduced type 1 (Th1) cytokine responses in C-C chemokine receptor 2 knockout mice. *J Clin Invest* 100: 2552–2561, 1997.
2. **Braganza JM, Lee SH, McCloy RF, McMahon MJ.** Chronic pancreatitis. *Lancet* 377: 1184–1197, 2011.
3. **Elashoff M, Matveyenko AV, Gler B, Elashoff R, Butler PC.** Pancreatitis, pancreatic, and thyroid cancer with glucagon-like peptide-1-based therapies. *Gastroenterology* 141: 150–156, 2011.
4. **Goto M, Nakano I, Kimura T, Miyahara T, Kinjo M, Nawata H.** New chronic pancreatitis model with diabetes induced by cerulein plus stress in rat. *Dig Dis Sci* 40: 2356–2363, 1995.
5. **Hedetoft C, Sheikh SP, Larsen S, Holst JJ.** Effect of glucagon-like peptide 1 (7–36) amide in insulin-treated patients with diabetes mellitus secondary to chronic pancreatitis. *Pancreas* 20: 25–31, 2000.
6. **Hiroyoshi M, Tateishi K, Yasunami Y, Maeshiro K, Ono J, Matsuoka Y, Ikeda S.** Elevated plasma levels of glucagon-like peptide-1 after oral glucose ingestion in patients with pancreatic diabetes. *Am J Gastroenterol* 94: 976–981, 1999.

7. **Lee YS, Park MS, Choung JS, Kim SS, Oh HH, Choi CS, Ha SY, Kang Y, Kim Y, Jun HS.** Glucagon-like peptide-1 inhibits adipose tissue macrophage infiltration and inflammation in an obese mouse model of diabetes. *Diabetologia* 55: 2456–2468, 2012.
8. **Li DS, Yuan YH, Tu HJ, Liang QL, Dai LJ.** A protocol for islet isolation from mouse pancreas. *Nat Protoc* 4: 1649–1652, 2009.
9. **Mantovani A, Sica A, Sozzani S, Allavena P, Vecchi A, Locati M.** The chemokine system in diverse forms of macrophage activation and polarization. *Trends Immunol* 25: 677–686, 2004.
10. **Mareninova OA, Sung KF, Hong P, Lugea A, Pandol SJ, Gukovsky I, Gukovskaya A.** Cell death in pancreatitis. *J Biol Chem* 281: 3370–3381, 2006.
11. **Mosser DM.** The many faces of macrophage activation. *J Leukoc Biol* 73: 209–212, 2003.
12. **Nakamura Y, Do JH, Yuan J, Odinokova IV, Mareninova O, Gukovskaya AS, Pandol SJ.** Inflammatory cells regulate p53 and caspases in acute pancreatitis. *Am J Physiol Gastrointest Liver Physiol* 298: G92–G100, 2010.
13. **Nathan JD, Romac J, Peng RY, Peyton M, Rockey DC, Liddle RA.** Protection against chronic pancreatitis and pancreatic fibrosis in mice over-expressing pancreatory secretory trypsin inhibitor. *Pancreas* 39: e24–e30, 2010.
14. **Nauck M, Frid A, Hermansen K, Shah NS, Tankova T, Mitha IH, Zdravkovic M, Düring M, Matthews DR; LEAD2 study group.** Efficacy and safety comparison of liraglutide, glimepiride, and placebo, all in combination with metformin, in type 2 diabetes: the LEAD (liraglutide effect and action in diabetes)-2 study. *Diabetes Care* 32: 84–90, 2009.
15. **Nyborg NC, Mølck AM, Madsen LW, Bjerre Knudsen L.** The human GLP-1 analog liraglutide and the pancreas: Evidence for the absence of structural pancreatic changes in three species. *Diabetes* 14: 1243–1249, 2012.
16. **Saeki K, Kanai T, Nakano M, Nakamura Y, Miyata N, Sujino T, Yamagishi Y, Ebinuma H, Takaishi H, Ona Y, Takeda K, Hozawa S, Yoshimura A, Hibi T.** CCL2-induced migration and SOCS3-mediated activation of macrophages are involved in cerulein-induced pancreatitis in mice. *Gastroenterology* 142: 1010–1020, 2012.
17. **Sasikala M, Talukdar R, Pavan Kumar P, Radhika G, Rao GV, Pradeep R, Subramanyam C, Nageshwar Reddy D.** β-Cell dysfunction in chronic pancreatitis. *Dig Dis Sci* 57: 1764–1772, 2012.
18. **Shiraishi D, Fujiwara Y, Komohara Y, Mizuta H, Takeya M.** Glicagon-like peptide-1 (GLP-1) induces M2 polarization of human macrophages via STAT3 activation. *Biochem Biophys Res Commun* 425: 304–308, 2012.
19. **Takada Y, Hisamatsu T, Kamada N, Kitazume MT, Honda H, Oshima Y, Saito R, Takayama T, Kobayashi T, Chinen H, Mikami Y, Kanai T, Okamoto S, Hibi T.** Monocyte chemoattractant protein-1 contributes to gut homeostasis and intestinal inflammation by composition of IL-10-producing regulatory macrophage subset. *J Immunol* 184: 2671–2676, 2010.
20. **Teratani T, Tomita K, Suzuki T, Oshikawa T, Yokoyama H, Shimamura K, Tominaga S, Hiroi S, Irie R, Okada Y, Kurihara C, Ebinuma H, Saito H, Hokari R, Sugiyama K, Kanai T, Miura S, Hibi T.** A high-cholesterol diet exacerbates liver fibrosis in mice via accumulation of free cholesterol in hepatic stellate cells. *Gastroenterology* 142: 152–164, 2012.
21. **Toft-Nielsen M, Madsbad S, Holst J.** Determinants of the effectiveness of glucagon-like peptide-1 in type 2 diabetes. *J Clin Endocrinol Metab* 86: 3853–3860, 2001.
22. **Tuo J, Rutledge BJ, Gu L, Fiorillo J, Lukacs NW, Kunkel SL, North R, Gerard C, Rollons BJ.** Abnormalities in monocyte recruitment and cytokine expression in monocyte chemoattractant protein 1-deficient mice. *J Exp Med* 187: 601–608, 1998.
23. **Wild S, Roglic G, Green A, Sicree R, King H.** Global prevalence of diabetes: estimates for 2000 and projections for 2030. *Diabetes Care* 27: 1047–1053, 2004.
24. **Yoo BM, Oh TY, Kim YB, Yeo M, Lee JS, Surh YJ, Ahn BO, Kim WH, Sohn S, Kim JH, Hahm KB.** Novel antioxidant ameliorates the fibrosis and inflammation of cerulein-induced chronic pancreatitis in a mouse model. *Pancreatology* 5: 165–176, 2005.
25. **Zion O, Genin O, Kawada N, Yoshizato K, Roffe S, Nagler A, Iovanna JL, Halevy O, Pines M.** Inhibition of transforming growth factor b signaling by Halofugione as a modality for pancreas fibrosis prevention. *Pancreas* 38: 427–435, 2009.

The FASEB Journal • Research Communication

The hydrolase DDAH2 enhances pancreatic insulin secretion by transcriptional regulation of secretagogin through a Sirt1-dependent mechanism in mice

Kazuhiro Hasegawa,* Shu Wakino,*,[1] Masumi Kimoto,[†] Hitoshi Minakuchi,* Keiko Fujimura,* Koji Hosoya,* Motoaki Komatsu,* Yuka Kaneko,* Takeshi Kanda,* Hirobumi Tokuyama,* Koichi Hayashi,* and Hiroshi Itoh*

*Department of Internal Medicine, School of Medicine, Keio University, Tokyo, Japan; and [†]Department of Nutritional Science, Okayama Prefectural University, Okayama, Japan

ABSTRACT **The role of dimethylarginine dimethylaminohydrolase 2 (DDAH2) in glucose metabolism is unknown. Here, we generated DDAH2 transgenic (Tg) mice. These mice had lower plasma glucose levels (60 min: 298±32 *vs.* 418±35 mg/dl; 120 min: 205±15 *vs.* 284±20 mg/dl) and higher insulin levels (15 min: 2.1±0.2 *vs.* 1.5±0.1 ng/ml; 30 min: 1.8±0.1 *vs.* 1.5±0.1 ng/ml) during intraperitoneal glucose tolerance tests when fed a high-fat diet (HFD) compared with HFD-fed wild-type (WT) mice. Glucose-stimulated insulin secretion (GSIS) was increased in Tg islets by 33%. Pancreatic asymmetrical dimethylarginine, nitric oxide, and oxidative stress levels were not correlated with improvements in insulin secretion in Tg mice. Secretagogin, an insulin vesicle docking protein, was up-regulated by 2.7-fold in Tg mice and in pancreatic MIN-6 cells overexpressing DDAH2. GSIS in MIN-6 cells was dependent on DDAH2-induced secretagogin expression. Pancreatic Sirt1, DDAH2, and secretagogin were down-regulated in HFD-fed WT mice by 70, 75, and 85%, respectively. Overexpression of Sirt1 overexpression by 3.9-fold increased DDAH2 and secretagogin expression in MIN-6 cells by 3.2- and 2.5-fold, respectively. DDAH2 overexpression improved GSIS in pancreas-specific Sirt1-deficient mice. In summary, the Sirt1/DDAH2/secretagogin pathway is a novel regulator of GSIS.—Hasegawa, K, Wakino, S., Kimoto, M, Minakuchi, H., Fujimura, K., Hosoya, K., Komatsu, M., Kaneko, Y., Kanda, T., Tokuyama, H., Hayashi, K., Itoh, H. The hydrolase DDAH2 enhances pancreatic insulin secretion by transcriptional regulation of secretagogin through a Sirt1-dependent mechanism in mice. *FASEB J.* 27, 2301–2315 (2013). www.fasebj.org**

Key Words: β cells · glucose-stimulated insulin secretion · glucose tolerance · knockout · overexpression

TYPE 2 DIABETES MELLITUS (T2DM) is one of the most serious metabolic disorders and is predicted to affect millions of people worldwide (1). T2DM is characterized by insulin resistance and impaired glucose-stimulated insulin secretion (GSIS). Several factors are involved in the pathogenesis of insulin resistance, including a reduction in nitric oxide (NO) bioavailability and knockdown of NO synthase (NOS) (2). However, the effects of NO on pancreatic insulin secretion are controversial, as some researchers reported that neuronal NOS (3) and inducible NOS (iNOS; ref. 4) in islets suppress GSIS, whereas others reported that neuronal NOS enhances GSIS (5).

Asymmetrical dimethylarginine (ADMA) is an endogenous inhibitor of NOS and is associated with hypertension (6). Intriguingly, insulin resistance and T2DM are associated with elevated plasma ADMA levels (7). ADMA is degraded by the enzyme dimethylargin-

Abbreviations: ADMA, asymmetrical dimethylarginine; AP, activator protein; BESTO, β-cell-specific Sirt1-overexpressing; CBP, Ca^{2+}-binding protein; CM-H2DCFDA, 5-(and-6)-chloromethyl-2′,7′-dichlorodihydrofluorescein diacetate acetyl ester; CREB, cAMP response element-binding protein; DAF-2-DA, diaminofluorescein-2-diacetate; DDAH, dimethylarginine dimethylaminohydrolase; ELISA, enzyme-linked immunosorbent assay; EMSA, electrophoretic mobility shift assay; GSIS, glucose-stimulated insulin secretion; HFD, high-fat diet; IGTT, intraperitoneal glucose tolerance test; IITT, intraperitoneal insulin tolerance test; IL, interleukin; iNOS, inducible nitric oxide synthase; KO, knockout; LFD, low-fat diet; NO, nitric oxide; NOS, nitric oxide synthase; PKA, protein kinase A; RIP, rat insulin promoter; ROS, reactive oxygen species; siRNA, small interfering RNA; SNAP-25, 25-kDa synaptosome-associated protein; T2DM, type 2 diabetes mellitus; Tg, transgenic; TORC1, CREB-regulated transcription coactivator 1; UCP2, uncoupling protein2; VEGF, vascular endothelial growth factor; WT, wild type

[1] Correspondence: Department of Internal Medicine, School of Medicine, Keio University, 35 Shinanomachi, Shinjuku-ku, Tokyo 160-8582, Japan. E-mail: shuwakino@z8.keio.jp.

doi: 10.1096/fj.12-226092

This article includes supplemental data. Please visit *http://www.fasebj.org* to obtain this information.

ine dimethylaminohydrolase (DDAH). There are two isoforms of DDAH, DDAH1 and DDAH2, which have divergent functions (6), including reducing ADMA levels and increasing NO levels. Both isoforms also act in an ADMA-independent manner. We previously reported that DDAH2 binds directly to protein kinase A (PKA), which activates the promoter of the vascular endothelial growth factor (VEGF) gene through an Sp1 site (8).

The physiological functions of DDAH1 were elucidated in studies of transgenic (Tg) mice overexpressing DDAH1 (9) and in DDAH1-knockout (KO) mice (10). In terms of insulin resistance, it was reported that insulin resistance was improved in DDAH1 Tg mice fed a normal diet (9). We have generated DDAH2 Tg (hereafter Tg) mice and previously reported that coronary atherosclerosis was alleviated in these mice as compared with wild-type (WT) mice (11). However, the role of DDAH2 in insulin resistance or glucose metabolism remains unknown. Therefore, the aim of this study was to examine the role of DDAH2 in glucose metabolism in mice and to identify the potential signaling pathways by which DDAH2 may regulate glucose metabolism. This study showed that DDAH2 overexpression in islets may improve GSIS by transcriptionally activating secretagogin expression *via* Sp1 in two animal models with impaired GSIS. Furthermore, Sirt1 transcriptionally regulates the DDAH2/secretagogin pathway. Our results suggest that DDAH2 offers a novel therapeutic target for T2DM by reversing high-fat diet (HFD)-induced impairments in GSIS.

MATERIALS AND METHODS

Animals and metabolic analysis

All mice were raised on a C57BL/6 genetic background. All experimental procedures were approved by the Institutional Animal Care and Use Committee of Keio University School of Medicine. DDAH2 Tg mice were generated as described previously (11). DDAH2 Tg mice and WT mice (n=8) were fed a low-fat diet (LFD; CE-2; Clea Japan, Tokyo, Japan) or an HFD (HFD-32; Clea Japan) for 12 wk. Metabolic parameters were determined using an Oxymax (Columbus Instruments, Columbus, OH, USA). Intraperitoneal glucose tolerance tests (IGTTs), intraperitoneal insulin tolerance tests (IITTs), and plasma biochemical tests were conducted as described previously (12). In the IGTT, the mice were denied access to food overnight (12 h) and then intraperitoneally injected with glucose at a dose of 1 g glucose/kg body weight. Blood glucose levels were measured before glucose injection and at 15, 30, 60, and 120 min after injection. In the IITT, the mice were denied access to food overnight (12 h) and then intraperitoneally injected intraperitoneally with 0.1 U/ml insulin (Humulin R; Eli Lilly, Indianapolis, IN, USA) in sterile PBS at a dose of 0.5 U insulin/kg body weight. Blood glucose levels were measured before and at 15, 30, 60, and 90 min after insulin injection. Plasma and tissue concentrations of ADMA were measured by HPLC (11).

Islet studies

Islet size and number were determined by computer-aided morphometric analysis (13). Pancreatic insulin content was measured using a rat/mouse insulin enzyme-linked immunosorbent assay (ELISA) kit (Linco Research, St. Charles, MO, USA). Immunofluorescence was performed with affinity-purified anti-insulin (Dako, Tokyo, Japan), anti-DDAH2 (provided by M.K.), and anti-secretagogin (Abcam, Cambridge, MA) antibodies. Immunoblotting was performed using antibodies against DDAH2 (provided by M.K.), secretagogin (Abcam), Sirt1 (Millipore, Bedford, MA, USA) and β-actin (Abcam). Gene expression levels of DDAH2, secretagogin, β-actin, insulin 1, and insulin 2 were determined by real-time PCR with the following primers (forward and reverse): DDAH2, GGTTGATGGAGTGCGTAAAGC and TCCACAATTCGGAGTCCCAA; secretagogin, CCCAGAAGTGGATGGATTTG and GTTGGGGATCAGGGGGTTTAT; β-actin, TGCTCTGGCTCCTAGCACCATGAAGATCAA and AAACGCAGCTCAGTAACAGTCCGCCTAGAA; insulin 1, CTGCTGGCCCTGCTTGC and GGGTCGAGGTGGGCCTT; insulin 2, CCTGCTGGCCCTGCTCTT and GGCTGGGTAGTGGTGGGTCTA.

Islet function studies

Islets were isolated by collagenase digestion, and GSIS was determined as described previously (14). Insulin levels were determined using an ELISA kit (Linco Research). ATP levels were measured using an ATP bioluminescent assay kit (Sigma, St. Louis, MO, USA). Ca^{2+} concentrations were measured using the Ca^{2+}-sensitive dye fluo-4 AM (Invitrogen, Carlsbad, CA, USA). Docked insulin granules were counted as described previously (15). Given their average diameter of 350 nm, secretory granules whose centers were located within 100–200 nm of the β-cell membrane were considered docked. Distances were determined by drawing a straight line from the granule center to the nearest plasma membrane (16).

DNA microarray analysis

Mice in the WT + LFD and Tg + LFD groups were killed at 20 wk of age. Tissues were immediately prepared for total RNA isolation and subjected to Affymetrix Mouse Genome 430 2.0 microarray chip analysis using standard protocols (Affymetrix, Santa Clara, CA, USA; http://www.affymetrix.com). Genes were excluded when the signal strength was not significantly greater than the background value or when their expression did not reach a threshold value for reliable detection (P<0.05) in all 3 independent studies. Genes were also excluded if the expression level did not differ by ≥3-fold or ≤0.33-fold between the WT + STZ and Tg + STZ groups. The remaining genes were subjected to nonparametric Welch t tests and are reported with their respective fold changes and P values.

Cell culture and transfection

MIN-6 cells were cultured as described previously (17). Murine DDAH2 cDNA was prepared, and the cells were treated with small interfering RNAs (siRNAs) targeting secretagogin (Santa Cruz Biotechnology, Santa Cruz, CA, USA), as described previously (8). siRNA for green fluorescent protein (5′-GGCTACGTCCAGCAGCGCACC-3′) mRNA was used as a negative control. The Sirt1 expression vector was cloned and transfected as described previously (18).

Determination of reactive oxygen species (ROS) and NO levels in islets

ROS levels were measured using the fluorescent probe 5-(and-6)-chloromethyl-2′,7′-dichlorodihydrofluorescein diacetate acetyl ester (CM-H2DCFDA; Invitrogen). NO levels were detected using diaminofluorescein-2-diacetate (DAF-2-DA; Invitrogen).

Generation of Sirt1 β cell-specific conditional-KO mice

Mice heterogeneous for the floxed Sirt1 allele ($Sirt1^{+/-}$) raised on a C57BL/6J background were kindly provided by Leonard Guarente (Massachusetts Institute of Technology, Cambridge, MA, USA; ref. 19). $Sirt1^{+/-}$ mice were bred with mice carrying the rat insulin promoter-Cre recombinase (RIP-Cre) gene on a C57BL/6J background (Jackson Laboratory) for β-cell-specific Sirt1-KO (RIP-Cre/Sirt1 *lox/lox*; RIP-$Sirt1^{+/-}$) mice. Male F2 offspring littermates derived from crosses between male F1 RIP-$Sirt^{+/-}$ mice and female F1 DDAH2 Tg mice were analyzed in the DDAH2 rescue experiments. Mice of each genotype, including WT littermates, were fed the LFD for 12 wk.

Luciferase assays and electrophoretic mobility shift assays (EMSAs)

A 1583-bp fragment (−1525 to +53) of the 5′ flanking region of the murine secretagogin gene was isolated from the murine BAC genomic clone using the restriction endonucleases *Ssp*I and *Bbs*I. Plasmids −680, −450, −346, and −84 Luc were made by subcloning the *Msp*I, *Ms*II, *Mae*III, and *Bse*PI inserts from −1525 Luc. These secretagogin/pGL3 plasmids (−1525 Luc, −680 Luc, −450 Luc, −346 Luc, and −84 Luc) containing the mouse secretagogin promoter sequences between −1525, −680, −450, −346, and −84 and +53 were fused to a pGL3 vector, a firefly luciferase reporter plasmid, and were transfected using Lipofectamine 2000 (Invitrogen). The DDAH2 expression plasmid and pRL-CMV (*Renilla* luciferase reporter vector; Promega, Madison, WI, USA) were cotransfected into cells. Similarly, a 1345-bp fragment (−1344 to +1) of the 5′ flanking region of the murine DDAH2 gene was isolated from the murine BAC genomic clone using the restriction endonucleases *Apo*I and *Sal*I. Plasmids −917, −648, −440, and −109 Luc were made by subcloning the *Pst*I, *Pfl*FI, *Ahd*I, and *Nsp*I inserts from −1344 Luc. These DDAH2/pGL3 plasmids (−1344 Luc, −917 Luc, −648 Luc, −440 Luc, and −109 Luc) containing the mouse DDAH2 promoter sequences between −1344, −917, −648, −440, and −109 and +1 were fused to a pGL3 vector, a firefly luciferase reporter plasmid and transfected using Lipofectamine 2000 (Invitrogen). The Sirt1 expression plasmid and pRL-CMV (*Renilla* luciferase reporter vector; Promega) were cotransfected into cells. Luciferase activity was measured as described previously (8). The EMSAs were performed using an EMSA kit (Panomics, Redwood City, CA, USA) and a nuclear extraction kit (Panomics), as described previously (8). The antibodies for Sp1 (07-645) and cAMP response element-binding protein (CREB; 06-863) were purchased from Millipore. Previous reports (20, 21) using the same antibodies revealed significant attenuation of protein binding to the Sp1 or CREB oligonucleotides as compared with a control antibody, but no supershifted bands were observed.

Statistical analysis

Data are expressed as means ± SE. Data were analyzed by 1- or 2-way ANOVA, as appropriate, followed by Bonferroni's multiple-comparison *post hoc* test. Values of $P < 0.05$ were considered statistically significant.

RESULTS

GSIS is enhanced in DDAH2 Tg mice

We first examined the effects of systemic DDAH2 overexpression (**Fig. 1**). WT and DDAH2 Tg (Tg) mice were fed an LFD or an HFD. In WT and Tg mice, weight gain, adipocyte size, and serum lipid levels were significantly greater in HFD-fed mice than in LFD-fed mice, although there were no differences between the WT and Tg mice fed either diet (Supplemental Fig. S1). At 20 wk of age, the body weights of WT and Tg mice fed the LFD were 38.0 ± 4.1 and 38.1 ± 5.0 g, respectively, while those of WT and Tg mice fed the HFD were 46.4 ± 6.0 and 45.9 ± 5.8 g, respectively. In LFD-fed mice (Fig. 1*A*, *B*), blood glucose and plasma insulin levels during the IGTT were not significantly different between WT and Tg mice. However, in HFD-fed mice (Fig. 1*C*, *D*), blood glucose levels were significantly lower in Tg mice than in WT mice at 60 and 120 min after the glucose load (Fig. 1*C*, top panel). Insulin levels at 15 and 30 min after the glucose load were significantly greater in HFD-fed Tg mice than in HFD-fed WT mice (Fig. 1*C*, bottom panel). There were no differences in ITT results between Tg and WT mice fed the HFD (Fig. 1*D*). These results indicate that insulin secretion was enhanced in HFD-fed Tg mice compared with that in HFD-fed WT mice, although insulin sensitivity was not improved in Tg mice. Glucose and insulin levels in the fed and unfed states were higher in HFD-fed mice than in LFD-fed mice in both genotypes (Fig. 1*E*). In the unfed state, glucose and insulin levels were similar between WT and Tg mice fed with either diet. In the fed state, glucose levels were lower and insulin levels were higher in HFD-fed Tg mice than in HFD-fed WT mice (Fig. 1*E*, bottom panel).

To identify the mechanisms involved in the amelioration of glucose metabolism in Tg mice, we examined islet structure and function. The numbers of islets were not significantly different between WT and Tg mice fed either diet (**Fig. 2*A***). Although islet size was greater in HFD-fed mice, there were no differences in islet size between WT and Tg mice (Fig. 2*B*). Insulin content in isolated islets was not significantly different between Tg and WT mice fed either diet (Fig. 2*C*). GSIS following exposure to 16.7 mM glucose was impaired in islets isolated from HFD-fed WT mice compared with islets from LFD-fed WT mice, consistent with previous reports showing that prolonged exposure to HFD exhausts individual islets and ultimately blunts insulin release (4). GSIS was significantly higher in Tg mice than in WT mice fed either diet (Fig. 2*D*). To explore the mechanism responsible for the enhanced GSIS in Tg mice, we measured glucose-induced Ca^{2+} release (Fig. 2*E*) and ATP production (Fig. 2*F*). Although

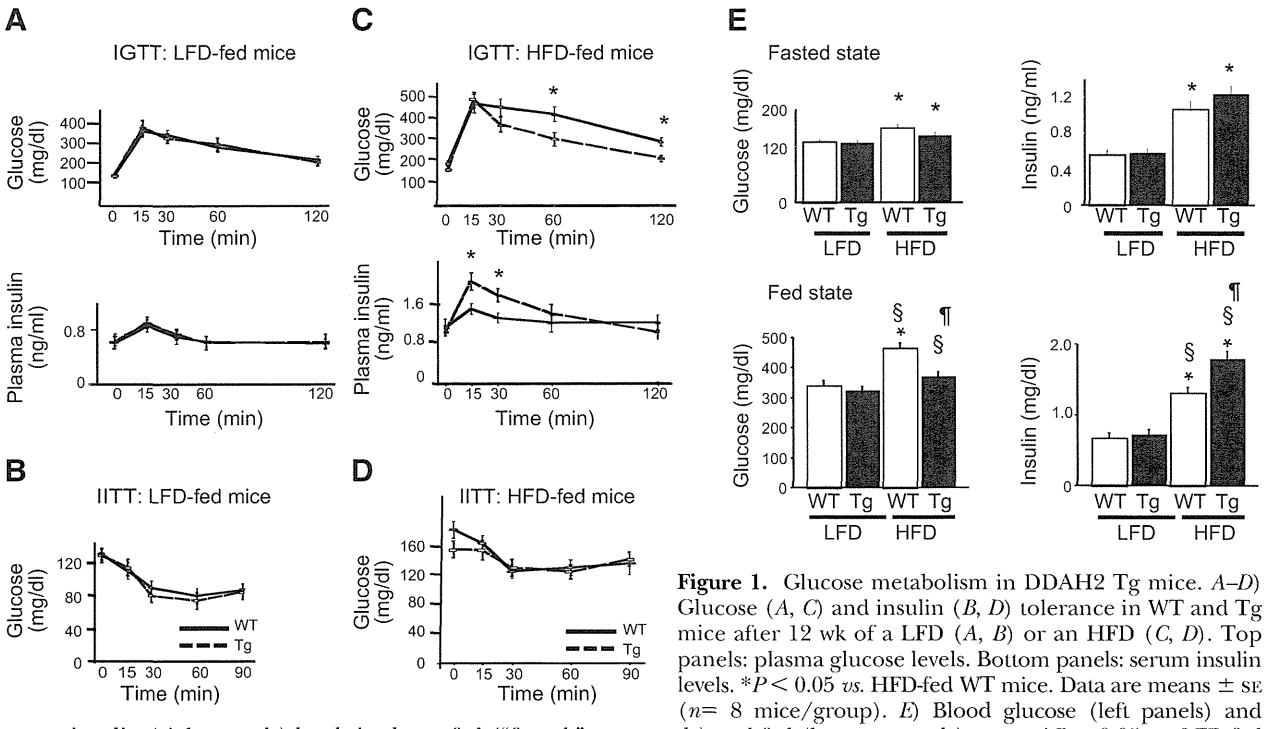

Figure 1. Glucose metabolism in DDAH2 Tg mice. *A–D*) Glucose (*A*, *C*) and insulin (*B*, *D*) tolerance in WT and Tg mice after 12 wk of a LFD (*A*, *B*) or an HFD (*C*, *D*). Top panels: plasma glucose levels. Bottom panels: serum insulin levels. $^{*}P < 0.05$ *vs.* HFD-fed WT mice. Data are means ± SE ($n = 8$ mice/group). *E*) Blood glucose (left panels) and serum insulin (right panels) levels in the unfed ("fasted;" top panels) and fed (bottom panels) states. $^{*}P < 0.05$ *vs.* LFD-fed WT mice; $^{\S}P < 0.05$ *vs.* LFD-fed Tg mice; $^{\P}P < 0.05$ *vs.* HFD-fed WT mice ($n = 4$ mice/group).

exposure to 16.7 mM glucose increased islet Ca^{2+} release and ATP content compared with 2.8 mM glucose in both Tg and WT mice, these parameters did not differ between WT and Tg mice. Finally, we counted the number of docked insulin granules. As shown in Fig. 2*G*, there were fewer docked insulin granules in HFD-fed WT mice than in LFD-fed WT mice. However, the number of docked granules was greater in Tg mice than in WT mice fed either diet. These results indicate that DDAH2 overexpression in the Tg mice ameliorated HFD-induced glucose intolerance by increasing both GSIS and the number of docked insulin granules.

DDAH2 is the dominant isoform in mouse islets

Our Tg mice showed increased GSIS and numbers of docked insulin granules, which indicates that DDAH2 plays a pivotal role in regulating insulin secretion. Therefore, we next performed immunohistochemistry to determine the relative expression levels of DDAH1 and DDAH2 in whole islets from C57BL6 mice. We found that DDAH2 protein was constitutively expressed in the islets, whereas DDAH1 protein was hardly detected (**Fig. 3*A***). These results are consistent with the mRNA expression levels of DDAH1 and DDAH2 in the pancreas (Fig. 3*B*).

DDAH2 affects GSIS independently of pancreatic NO metabolism

We next examined whether NO metabolism was altered in Tg mice. Immunofluorescence studies confirmed that DDAH2 was decreased in the islets from HFD-fed WT mice, but this decrease was rescued in the islets from HFD-fed Tg mice (Fig. 3*C*). The mRNA expression level of DDAH2 was also decreased by the HFD, but it was reversed by DDAH2 overexpression. The mRNA expression levels of insulin 1 and insulin 2 were unaffected (Fig. 3*D*). These changes in DDAH2 expression were compatible with the changes in GSIS in Tg mice, suggesting that DDAH2 is involved in GSIS in pancreatic β cells. Although the HFD increased pancreatic ROS (Fig. 3*E*) and NO (Fig. 3*F*) levels, there were no differences in their levels between WT and Tg mice fed either diet, indicating that pancreatic NO and ROS do not contribute to the difference in insulin secretion between WT and Tg mice. Although pancreatic ADMA levels were lower in TG mice than in WT mice, they were not affected by the HFD (Fig. 3*G*). These data indicate that the pancreatic changes in ADMA, NO, or ROS levels are not associated with the HFD-induced changes in GSIS in Tg or WT mice. Taken together, these results indicate that DDAH2 affects GSIS *via* an ADMA-independent mechanism.

Secretagogin is involved in insulin secretion in DDAH2 Tg mice

To determine the molecular mechanism involved in the enhanced insulin secretion in HFD-fed Tg mice, we performed DNA microarray analysis to examine islet gene expression profiles. The expression levels of several genes associated with insulin vesicle docking, including secretagogin, Rab3d, and Rab27, were higher

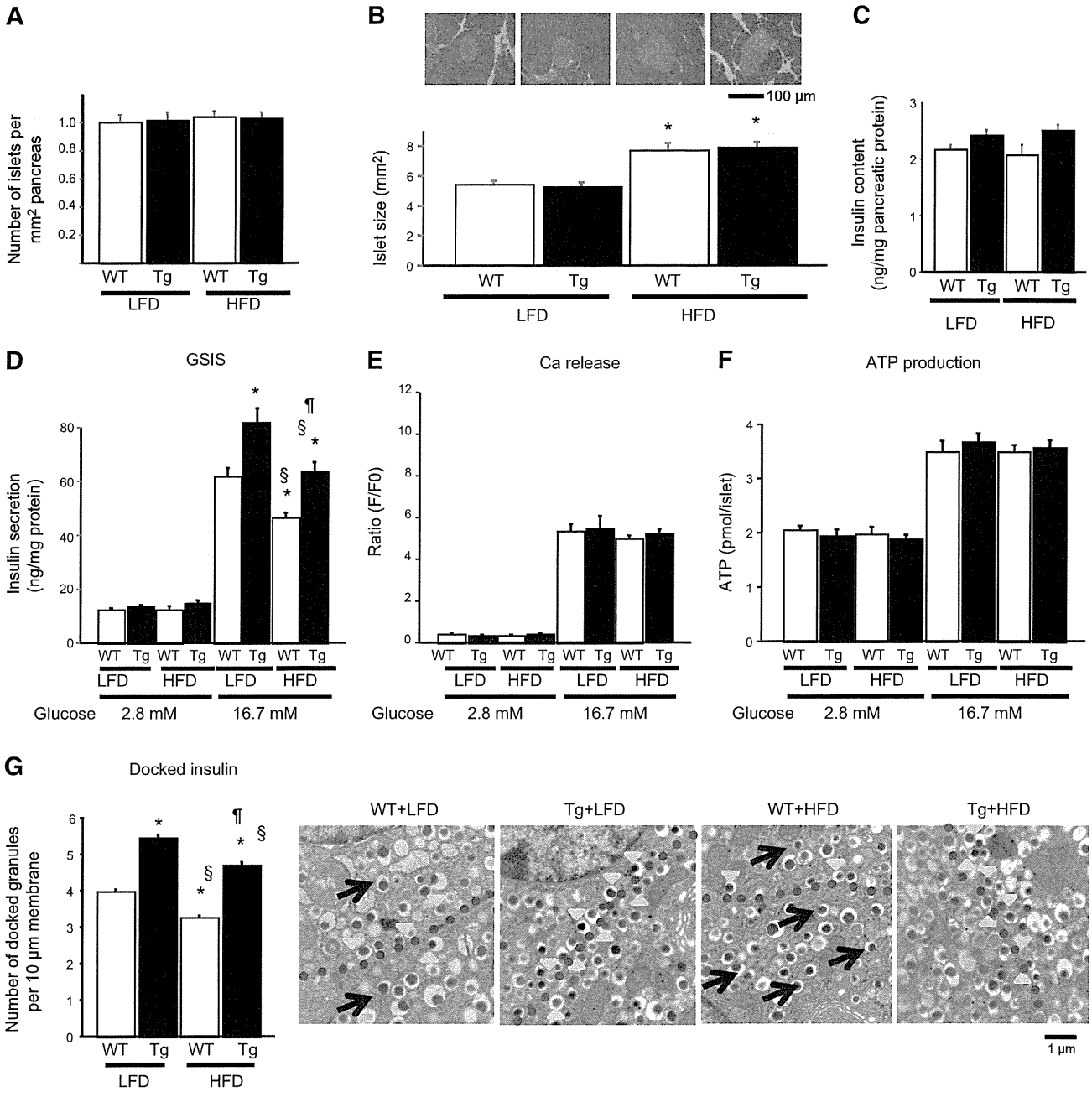

Figure 2. Islet morphology and function in DDAH2 Tg mice. *A*) Number of islets per square millimeter of pancreas tissue (n=8 mice/group). *B*) Islet size determined by immunohistochemistry with anti-insulin antibodies. Top panels show representative images. Scale bar = 100 µm. View = ×100. $^{*}P < 0.05$ *vs.* LFD-fed WT mice (n=8 mice/group). *C*) Pancreatic insulin content was determined using acid–ethanol extracts (n=8 mice/group) and is expressed as nanograms of insulin per microgram of pancreatic protein. *D–F*) Islets cultured overnight were incubated for 60 min in Krebs-Ringer bicarbonate buffer with 2.8 or 16.7 mM glucose. *D*) GSIS in isolated islets (n=8 mice/group). *E*) Ca^{2+} response to glucose. Islets attached to coverslips were loaded with 10 µM Fluo-4 AM and placed in a perfusion chamber, and Ca^{2+} concentrations were measured by confocal microscopy as the fluorescence intensity after stimulation (F)/fluorescence intensity at rest (F_0). Values are expressed as means ± SE. (n=8 mice/group), *F*) ATP concentrations in response to glucose. (n=8 mice/group). *G*) Number of docked insulin granules counted under electron microscopy. At least 15 cells were analyzed in each group (5 cells in each of 3 animals). Dashed lines indicate the plasma membrane. Arrows and arrowheads indicat representative undocked and docked granules, respectively. $^{*}P < 0.05$ *vs.* LFD-fed WT mice; $^{\S}P < 0.05$ *vs.* LFD-fed Tg mice; $^{\P}P < 0.05$ *vs.* HFD-fed WT mice (n=8 mice/group).

in Tg mice than in WT mice (Supplemental Table S1). However, there were no differences in the expression levels of genes related to insulin signaling, transcription factors, or apoptosis. Secretagogin is an EF-hand Ca^{2+}-binding protein (CBP) that was originally cloned from pancreatic β cells (22). Since a previous study (23)